Elucidating the Role of UbE2K in the Post-Translational Regulation of the Tumor Suppressor PTEN

A Thesis
Presented in Partial Fulfillment of the Requirements for
Graduation with Research Distinction from the School of Health and Rehabilitation Sciences of The Ohio State University

Matthew Robert Lordo

The Ohio State University
School of Health and Rehabilitation Sciences
Biomedical Sciences Program
2016

Honors Thesis Examination Committee:
Dr. Sarmila Majumder, Advisor
Dr. Michael Ostrowski
Dr. Christopher Taylor

Table of Contents

Problem

The tumor suppressor phosphatase and tensin homolog deleted in chromosome ten (PTEN) is one of the most frequently altered genes in human cancer. Germline mutations in PTEN result in autosomal dominant hamartomatous syndromes, including Cowden Syndrome, a disease that carries an increased risk for breast, thyroid, and endometrial cancer. Although genetic and epigenetic alterations account for PTEN loss in many cancers, in breast cancer there is a very low incidence of mutation in *PTEN* [1]. Loss of PTEN has been shown to significantly increase the rate of tumor progression in multiple mouse models of breast cancer, including ErbB2 induced mammary tumorigenesis, and plays an important role in both the epithelial and stromal compartments [2]. These data also correlate with human disease progression, as our studies demonstrate that patients with low PTEN protein levels have worse disease outcome compared to patients with high levels of PTEN protein (unpublished data). However, *PTEN* mRNA levels in this patient cohort are not predictive of disease outcome. Our observation that 30-40% of the breast cancer patients have a reduction in PTEN protein levels without significant alteration of its expression suggests that post-translational events play a key role in regulating PTEN protein levels in breast cancer. Thus, a global shRNA screen to identify putative regulators of PTEN protein was undertaken in the laboratory. A subset of the identified PTEN degradome are components of the ubiquitin-proteasome pathway. Treatment of cells with the proteasome inhibitor MG132 results in an increase in total PTEN protein, supporting our observation. We chose to study one of these genes, ubiquitin conjugating enzyme E2K (UbE2K), to elucidate its mechanism of action in regulating PTEN protein levels.

Background

PTEN

Phosphatase and tensin homolog deleted in chromosome 10 (PTEN) was first described in 1997 as a dual lipid and protein phosphatase that selectively dephosphorylates the molecule phosphatidylinositol (3,4,5)-trisphosphate to phosphatidylinositol (4,5)-bisphosphate (PIP_3 to PIP_2) [3,4]. Other targets of

PTEN's phosphatase activity include the proteins IRS1, involved in the IGF signaling pathway, and Dishevelled, a member of the Wnt signaling pathway [5, 6]. *PTEN* is located at locus 10q23 in human and codes for a 403 amino acid protein product. It is composed of five functional domains: a phosphatidylinositol-4,5-bisphosphate [PtdIns(4,5)P_2]-binding domain (PBD), a phosphatase domain, a C2 domain, a carboxy-terminal tail and a PDZ-binding domain (**Figure 1**). Its lipid phosphatase activity

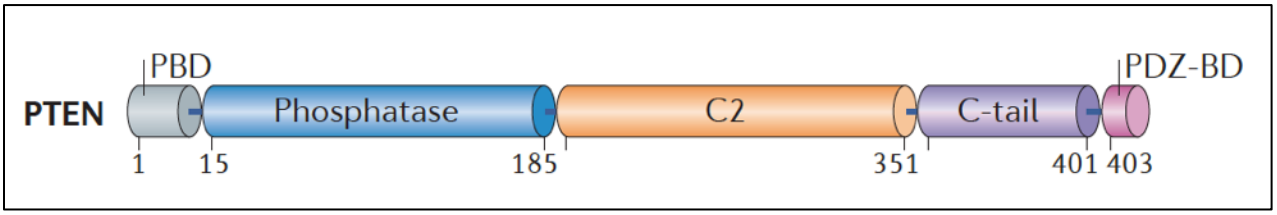

Figure 1 PTEN contains 5 domains that define its substrate specificity and function. Its enzymatic activity stems from its phosphatase domain, while the C2 domain forms its structural backbone [7].

is vital for its tumor suppressor activity by inhibiting AKT activation. Further studies have elucidated that PTEN is a haploinsufficient tumor suppressor, as loss of just one copy of the gene predisposes an individual to cancer and accelerates tumorigenesis [8]. This is well documented using mouse models of cancer including breast, pancreas, lung, colon, and gliomas models [reviewed in 9]**.** In hormone receptor negative breast cancer patients who had disease recurrence within the first 36 months of diagnosis, we observed a significant correlation between low levels of PTEN and worse clinical outcome compared to patients with high PTEN levels (**Figure 2A,** unpublished data). PTEN mRNA levels were not predictive of disease outcome in this patient cohort. There are several documented human diseases that result from loss of PTEN, including Cowden syndrome, Lhermitte-Duclos disease, Bannayan-Riley-Ruvalcaba syndrome, and Proteus and Proteus-like syndromes. Collectively, these diseases are known as PTEN hamartoma tumor syndromes. In mice, studies have shown that there is a large variation in phenotype depending on how Pten activity is affected [10]. Loss of either Pten's lipid or protein phosphatase activity leads to different phenotypes in mice compared to complete deletion or a catalytically inactive form of Pten. This offers a potential explanation for why loss of one tumor suppressor can produce such a diverse array of symptoms in patients.

Studies in the past have shown that PTEN is important in both the epithelial and stromal compartments in preventing tumor progression. Loss of PTEN in one compartment can influence several downstream events in the other, primarily resulting from cross-talk between the two compartments, aggravating tumorigenesis [11]. Thus, tumors and the surrounding stroma are able to co-evolve with each other, promoting further tumor growth. Therefore, it is important to study how PTEN levels are regulated in both the epithelium and surrounding stroma in order to have a comprehensive understanding of how this important tumor suppressor is regulated under normal condition and in a diseased state. A recent

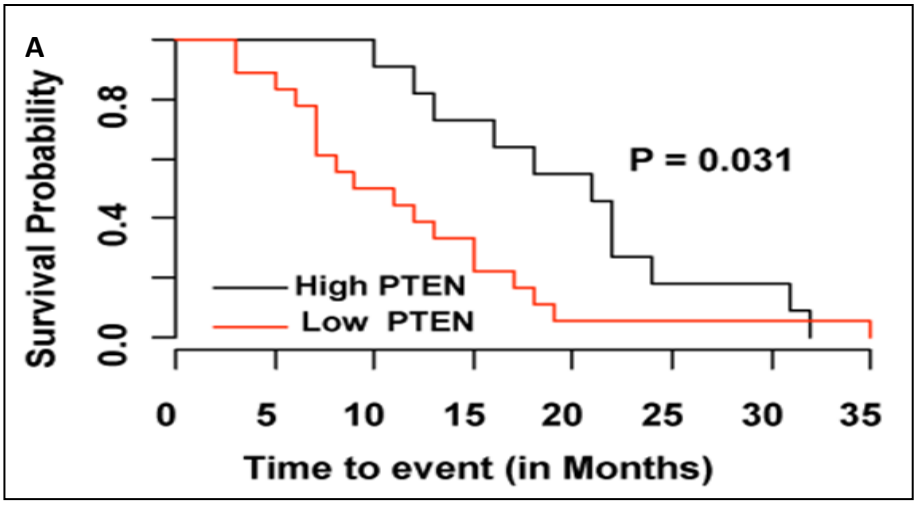

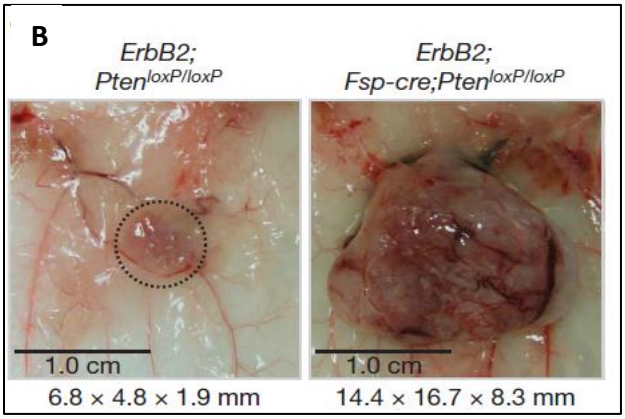

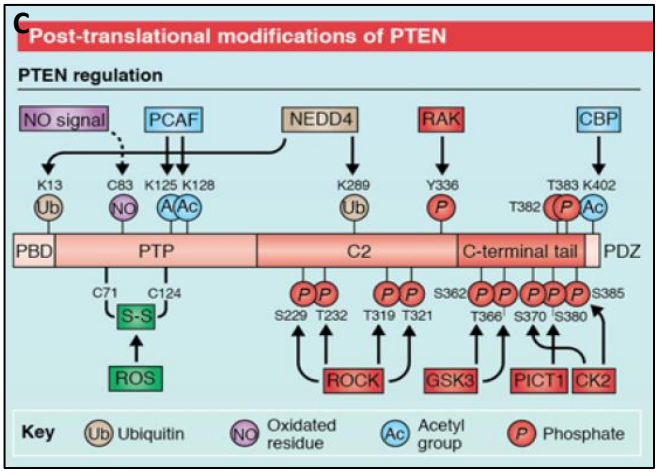

Figure 2 A). Low PTEN protein levels in triple negative breast cancer patients correlates strongly with worse disease outcome. B) Loss of Pten in stromal fibroblasts using an ErbB2 cancer model resulted in a significant increase in tumor growth rate [2]. C) PTEN is subject to multiple post-translational modifications including ubiquitination, SUMOylation, phosphorylation, and acetylation that it affects the protein's stability, localization and enzymatic activity [12].

study conducted in our laboratory highlighting the importance of stromal Pten in suppressing tumor formation utilized an ErbB2 driven mammary tumor model with deletion of Pten in the stromal fibroblasts [2]. Compared to mice with just the oncogenic driver, the concomitant loss of stromal Pten significantly increased tumor volume and grade (**Figure 2B**).

PTEN is subject to multiple post-translational modifications that can alter its activity, localization, and stability (**Figure 2C**). The primary post-translational modifications that affect PTEN protein stability include phosphorylation (**Figure 3**) and ubiquitination (discussed in detail below). Phopshorylation of PTEN by enzymes like GSK3β at Ser362 and Thr366 leads to inhibition of PTEN activity and has been implicated in the formation of gliomas [13]. Phosphorylated PTEN must become desphosphorylated before it is able to associate with membranes to exert its full functionality. PTEN is also subject to SUMOylation by molecules such as SUMO1 at Lys254 and Lys266 to regulate both PTEN activity and nuclear localization [14]. Acetylation of the residues between Lys125-128 in the phosphatase domain can lead to impairment of PTEN activity [15]. Finally, PTEN is subject to ubiquitination by many different ubiquitin ligases such as NEDD4 and MKRN1 with downstream effects ranging from proteasomal degradation to translocation [16, 17].

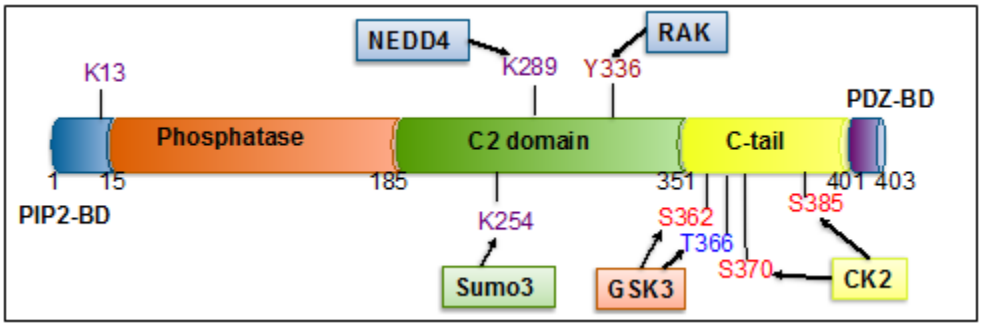

Figure 3 Several phosphorlyation sites have been mapped that either promote or protect PTEN from degradation. GSK3B–mediated phosphorylation at Ser362 and Thr366 is known to destabilize PTEN. In contrast, RAK mediated phosphorylation of PTEN at Tyr336, or Casein Kinase II-mediated phosphorylation at Ser370, Ser380, Thr382, Thr383 and Ser385 protects PTEN from degradation.

PI3K/AKT Pathway

The PI3K/AKT pathway plays a central role in regulating many cellular functions, including protein synthesis, cell survival and migration, cell division, and metabolism (**Figure 4**). Ligand-mediated activation of a receptor tyrosine kinase (RTK) leads to activation of PI3K which results in phosphorylation of the second messenger PIP_2 to PIP_3. PIP_3 promotes phosphorylation of AKT by activating PDK1 [18]. Phosphorylated AKT then signals to many downstream targets, promoting cell cycle progression and cell survival via inhibition of pro-apoptotic molecules. PTEN inhibits this pro-survival signal by dephosphorylating PIP_3, thereby attenuating p-AKT signaling. The PI3K-AKT pathway has been targeted to treat breast cancer patients, with some proven efficacy. Notable selective PI3K inhibitors used in breast cancer therapy include Buparlisib [19], Pilaralisib, and Pictilisib [reviewed in 20]. Our studies focus on an upstream inhibitor of this pathway, PTEN, that dephosphorylates the substrate of PI3K, PIP_3, to inhibit downstream AKT signaling.

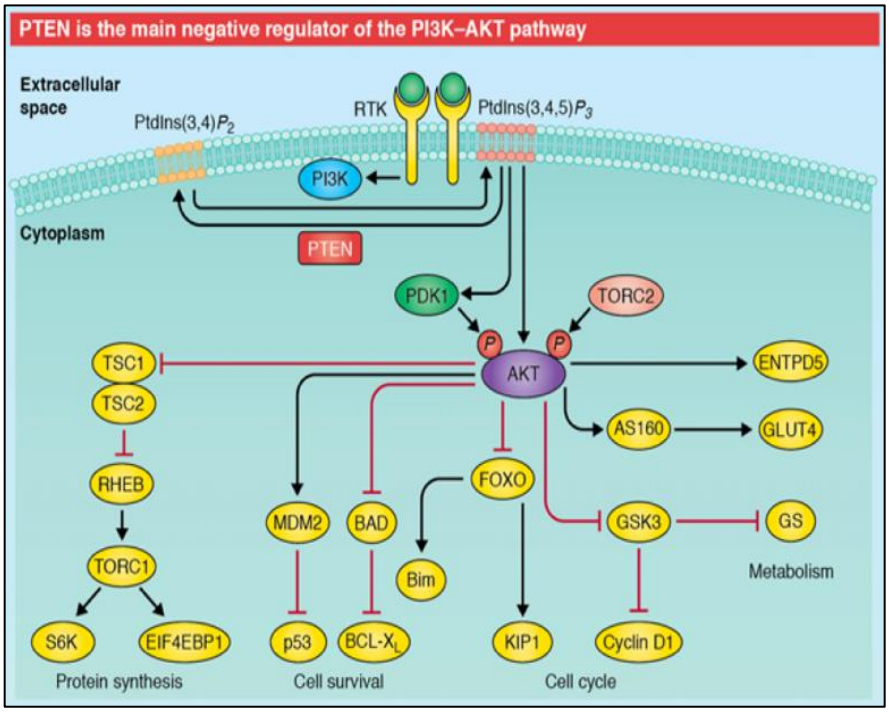

Figure 4 Schematic of the PI3K/AKT pathway. The second messenger PIP_2 is phosphorylated to PIP_3 by the enzyme PI3K. PIP_3 then leads to the phosphorylation of AKT, a kinase with many downstream targets, including the signal for cell division. PTEN acts as the main negative regulator of this pathway by selectively dephosphorylating PIP_3 to PIP_2 [12].

Ubiquitin-Proteasome Pathway

The ubiquitin-proteasome pathway (UPP) is an important intracellular mediator of a diverse range of cellular functions. Ubiquitination alters protein stability, protein-protein interactions, protein activity, and subcellular localization, among other properties. The UPP involves three different enzymes that results in the covalent linkage of an ubiquitin molecule to the desired substrate (**Figure 5A**). E1 activating enzymes (1 enzyme) bind free ubiquitin through a thioester bond and transfer it to a cysteine residue in the active site of an E2 conjugating enzyme (~50 enzymes). These two molecules must dissociate before the E2 conjugating enzyme can associate with an E3 ubiquitin ligase (~500 enzymes). The E3 ligase binds to the substrate molecule and transfers the activated ubiquitin molecule to the substrate [reviewed in 21]. Furthermore, E2 conjugating enzymes that associate with E3 ligases containing a RING-domain are able to directly transfer the ubiquitin moiety to the substrate, using the E3 ligase for structural support [22]. For HECT-domain E3 ligases, the E2 enzyme transfers the ubiquitin moiety to the E3 ligase, which subsequently transfers it to the substrate. Substrate proteins can undergo mono-ubiquitination or poly-ubiquitination and can be linked through multiple different lysine residues on ubiquitin (**Figure 5B**). Of the seven Lys residues in ubiquitin (Ub), Lys48- and Lys11-linked ubiquitin chains target proteins for proteasomal degradation and Lys63-linked chains, in general, mediate recruitment of binding partners that orchestrate activation of different signaling pathways [23].

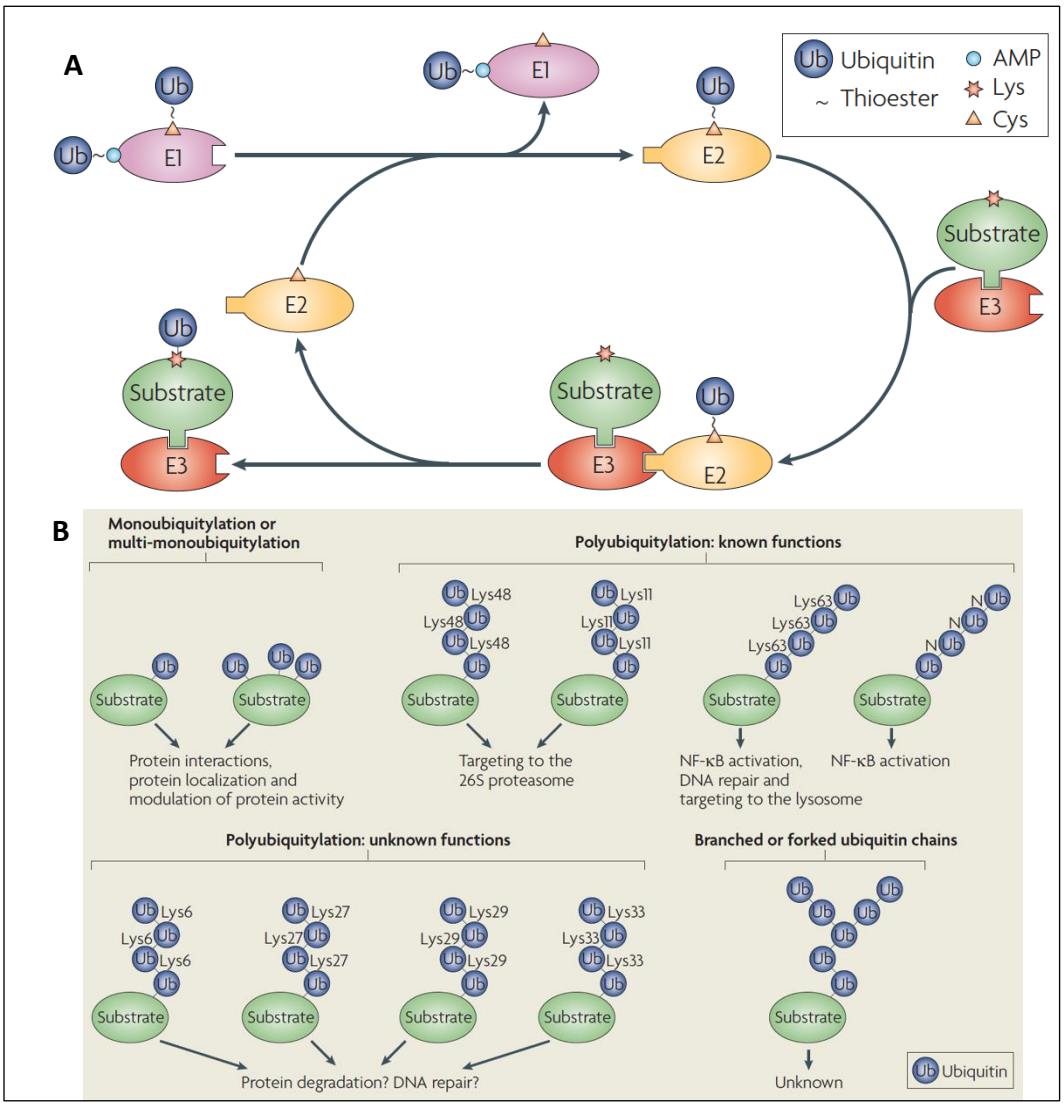

Figure 5 A) the ubiquitin-proteasome pathway involves 3 enzymes: E1 activating enzymes, E2 conjugating enzymes, and E3 ligases that cycle to produce ubiquitinated substrate based on the specificity of the E3. B) Different patterns of ubiquitination can result in different downstream effects, including proteasomal degradation or intracellular translocation [21].

UbE2K

Ubiquitin conjugating enzyme E2K was initially characterized in the brain, where it has particularly high expression levels in the frontal cortex and striatum, and is otherwise known as huntingtin-interacting protein 2 (HIP2) [24]. UbE2K selectively catalyzes the formation of Lys-48 linked ubiquitin chains, which promotes degradation of the substrate by the 26S-proteasome complex [25]. UbE2K has been shown to have some E3-independent activity, being able to generate unanchored polyubiquitin chains in the absence of an E3 ligase. However, this activity is dramatically increased in the presence of E3 ligases.

UbE2K *in vitro* can interact with RING-domain E3 ligases, such as the anaphase promoting complex or the BRCA1-BARD1 heterodimer to add polyubiquitin chains to pre-existing monoubiquitinated sites on substrates [26, 27]. As a consequence it regulates the proteasomal degradation of targeted substrates.

Proteasome-Targeted Therapies

One of the hallmarks of cancer is the loss of cell-cycle regulation that leads to hyperproliferation of cells. These transformed cells often overexpress many proteins, some misfolded, and thus have a large need for proteasomes to degrade them. Thus, tumor cells are sensitive to the levels of proteasomes present [28-30]. Pharmacologic inhibition of proteasome activity using drugs like Velcade has proven effective in hematopoietic cancers such as multiple myeloma [31, 32]; however there has been limited success in using this approach in solid tumors due to high toxicity. This could be attributed to less accessibility of the drug, requiring higher doses in solid tumors to demonstrate any efficacy. Current therapies aim to prevent the subunits of the 26S-proteasome from assembling by interfering with chaperones vital for their association [33, reviewed in 34]. The results of our studies hope to identify novel targets for inhibition to selectively increase PTEN levels by preventing its degradation by the proteasome.

Significance

Our basic understanding of the signaling pathways, components and physiological conditions that regulate PTEN protein stability is limited and poses a major challenge in the field. Because PTEN is implicated in a wide variety of cancers, unraveling the underlying mechanisms governing PTEN expression and stability is an important step to understand the basic mechanism of its regulation and in identifying targets for future therapies. Restoration of PTEN protein levels in tumor cells and in the surrounding microenvironment could slow the rate of tumor progression or even reverse the cancerous phenotype. This could offer cancer patients with limited treatment options, such as triple negative breast cancer patients, with new therapeutic options.

Hypotheses

As our screen identified UbE2K as a negative regulator of PTEN**, we hypothesize that depletion or targeted disruption of *UbE2K* in both *in vitro* and *in vivo* models will lead to increases in PTEN protein levels**. **We also hypothesize that UbE2K regulates PTEN through the UPP**. As we have previously shown that Pten levels in both mammary epithelium and stromal fibroblasts are important in preventing tumor development, we will study how loss of Ube2k in the epithelial and stromal compartments of mouse mammary gland affects its development and eventually mammary tumorigenesis.

Objectives

Objective 1. *Determine if depletion of the negative regulator UbE2K leads to increases in PTEN protein levels and study its underlying mechanism*

Objective 2. *Study the effects of Ube2k deletion in the mammary epithelium and stromal fibroblasts in mice*

Methodology and Rationale

Objective 1. *Determine if depletion of UbE2K, a negative regulator of PTEN leads to increases in PTEN protein levels and study its underlying mechanism*

For this study we used the normal human mammary epithelial cell line MCF10A. These cells were engineered to express the unstable $PTEN^{C124R}$ mutant that has a significantly shorter half-life compared to endogenous PTEN. We expressed this unstable mutant of PTEN with the rationale that the effect of depletion of a negative regulator on the mutant will be significantly amplified compared to endogenous PTEN. We used three different non-overlapping shRNAs targeting the UbE2K transcript to knockdown UbE2K. We then used quantitative polymerase chain reaction (qPCR) and sodium dodecyl sulfate polyacrylamide gel electrophoresis (SDS-PAGE) to assess the efficiency of the knockdown and to determine any changes in the endogenous and mutant PTEN protein levels compared to a negative control, expressing scrambled shRNA. To study the mechanism of PTEN degradation, we ectopically

expressed UbE2K and PTEN in HEK293t cells and conducted a co-immunoprecipitation to see if UbE2K and PTEN associate with each other in the same complex. We also conducted immunoprecipitation studies to assess changes in the ubiquitination profile of Pten upon *Ube2k* deletion using mouse embryonic fibroblasts (MEFs) isolated from wild type and *Ube2k* deleted mouse embryos.

Objective 2. *Study the effects of Ube2k deletion in the mammary epithelium and stromal fibroblasts in mice*

We generated *Ube2k* conditional knockout mice (*Ube2k*$^{fl/fl}$) using the Genetically Engineered Mouse Modeling core facility at the Ohio State University. We then bred these mice with mice expressing a Cre-recombinase for tissue specific deletion of *Ube2k*. To study the effects of loss of *Ube2k* in the stroma we used Fsp-Cre. This tissue-specific Cre was generated in the lab and is driven by the *Fsp (fibroblast specific protein)* promoter, which is primarily expressed in fibroblasts. We also crossed the *Ube2k*$^{fl/fl}$ mice with MMTV-Cre to study loss of *Ube2k* specifically in the mammary epithelium. This tissue-specific Cre is driven by the *MMTV (Mouse Mammary Tumor Virus)* promoter, which is expressed primarily in the mammary epithelium. We then aged these mice and harvested the mammary glands for immunohistochemistry (IHC), Carmine red staining, and Hematoxylin & Eosin (H&E) staining.

Materials and Methods

Cell Culture: MCF10A cells were grown in phenol-red (PR) containing DMEM/F12 media containing human EGF (20 ng/mL, Peprotech), insulin (10 µg/mL, Sigma), cholera toxin (100 ng/mL, Sigma), hydrocortisone (0.5 mg/mL, Sigma), horse serum (5%, Invitrogen), and penicillin/streptomycin (Invitrogen). Mouse embryonic fibroblasts, MB468, BT474, and T47D cell lines were cultured in PR-containing media supplemented with fetal bovine serum (10%, Sigma) and penicillin/streptomycin. Cells were maintained at 37°C and 5% CO_2.

Transfection: HEK293t cells were seeded in 60 mm dishes at a density of 1,000,000 cells. The following day, cells were transfected with the respective shRNA plasmid (2.5 µg, pGIPZ, Thermo),

psPAX2 (1.25 µg, packaging plasmid, Addgene), and pMD2.g (1.25 µg, envelope plasmid, Addgene) using JetPEI reagent (PolyPlus). The viral supernatant was harvested 48 hours later by filtering through a 0.45 µm filter. The supernatant was diluted 1:1 with 10% DMEM along with polybrene (8 µg/mL) and added to the target cells. After overnight incubation, the infection medium was changed to 10% DMEM and incubated for 48 hours. Following this incubation, puromycin was added to the media (2 µg/mL) for 1 week to select for infected cells. Infection efficiency was also tracked under a fluorescent microscope through the expression of GFP.

RNA: Cells were grown to 70-80% confluency and RNA was isolated using TRIzol reagent (Invitrogen) according to the manufacturer's protocol. cDNA was generated using a High Capacity Reverse Transcription kit (Applied Biosystems) according to the manufacturer's protocol. 2 µg of RNA were converted to cDNA. Real-time PCR (qPCR) was conducted using SYBR green SuperMix (BioRad). The primers used for qPCR are as follows:

Gene	Forward Primer (5'→3')	Reverse Primer (5'→3')
hPTEN	TACACATAGCGCCTCTGACTGG	TTGACCAATGGCTAAGTGAAGA
mPten	TTGACCAATGGCTAAGTGAAGA	TATACATAGCGCCTCTGACTGG
hUbE2K	CACCATATGAAGGAGGAAGA	TCGGGATTTTGTTTGTACTG
mUbe2k	GCGAGGAGACGAGCAAAAATC	CAAATAGCCCCTGTGACGGA
hRNF5	ATGTTTGGAGACTGCTCGGG	AATGGCTGGAATCCCCCTCT
GAPDH	TCCTGCACCACCAACTGCTTAG	TGCTTCACCACCTTCTTGATGTC
β-actin	TTTGAGACCTTCAACACCCCAGCC	AATGTCACGCACGATTTCCCGC

Table 1 Sequences of primers used to conduct qRT-PCR analysis. Primers were determined using the NCBI BLAST program.

Protein: whole cell lysates were prepared in radioimmunoprecipitation assay (RIPA) buffer (150 mM NaCl, 50 mM Tris-HCl pH 8.0, 1% NP-40, 0.05% Sodium Deoxycholate, 0.1% Sodium Dodecyl Sulfate) containing protease and phosphatase inhibitors. Lysates were incubated on ice for 30 minutes before being centrifuged. The clear supernatant was collected and protein concentration measured using the BCA protein assay kit (Pierce, Thermo Fisher). Whole cell lysates were separated on SDS-PAGE gels and proteins were transferred to PVDF membranes. After transfer, membranes were blocked for 30 minutes in 5% milk, 0.1% TBS-Tween and incubated in primary antibody overnight. The following day,

membranes were washed twice with 0.1% TBST before incubation in HRP-conjugated secondary antibody for one hour and developed using ECL reagent (Thermo).

Co-culture Assay: Breast cell lines expressing tetrameric Ds-Red (Clonetech) were plated in a 96-well plate containing Cultrex basement membrane extract (final concentration 3 mg/mL, Trevigen) along with patient-derived fibroblasts. Cells were plated in a 1:1 ratio (12,500 epithelial cells and 12,500 fibroblasts per well). PBS was added to the peripheral wells to maintain a constant humidity and prevent desiccation of the gel. The following day, 50 µL of phenol-red free DMEM was overlaid on the gel. Absorption readings were taken daily at 592 nm to monitor the growth curve of the Ds-red-tagged cancer cells.

Immunoprecipitation: Whole cell lysates were prepared as described above. 500 µg of protein was precleared using IgG/IgA beads (Millipore) for 30 minutes before being incubated with 4 µL of antibody overnight. The following day, IgG/IgA beads were added to the mixture for one hour before being washed three times. The immunoprecipitated complex was separated on a gradient SDS-PAGE gel (BioRad), transferred to a PVDF membrane, and probed with specific antibodies as described above. Antibodies used include: PTEN (Catalog # 9559L, Cell Signaling), UbE2K (Catalog # 8226S, Cell Signaling), GAPDH (Catalog # sc-25778, Santa Cruz), and β-actin (Catalog # A1978, Sigma).

Mouse Studies: All mouse experiments were conducted in accordance with the rules and guidelines of the Institutional Animal Care and Use Committee (IACUC) of the Ohio State University (Protocol # 2007A0239-R2). Mammary glands were harvested from the thoracic and inguinal regions and either fixed using 4% paraformaldehyde (PFA) for immunohistochemistry or Carnoy's fixative (60% ethanol, 30% chloroform, and 10% glacial acetic acid) for carmine red staining (0.2% carmine, 0.5% aluminum potassium sulfate, and 1 crystal of thymol). PFA-fixed samples were stored in 70% ethanol until further processing, while carmine-stained samples were washed in increasing concentration of ethanol (70% ethanol, 95% ethanol, and 100% ethanol, 1 hour each) and then stored in xylene.

Embryos used for IHC analysis were harvested at embryonic day 13.5 following observation of a plug in the mother. Genotyping was conducted by isolating DNA from the embryonic yolk sac following an

overnight digestion in lysis buffer (100 mM Tris-HCl pH 8.5, 5 mM EDTA, 0.2% SDS, 200 mM NaCl, 1 µg/mL proteinase K). Embryos and placenta were fixed in formalin for 48 hours and stored in ethanol prior to being sectioned and stained.

To isolate mouse embryonic fibroblasts, we harvested the uterus of the mother at embryonic day 13.5 and transferred it to sterile PBS in a laminar flow hood. The uterus was opened and each individual embryo was isolated using embryo scissors. The yolk sac was used for genotyping as described above. Visceral organs were removed and the embryo was then placed in an eppendorf and minced using a sterile scalpel. Trypsin was added to the embryos (500 µL, 0.05%) and the suspension was pipetted until homogenized. The suspension was then plated onto a 10 cm dish with additional trypsin (5 mL) and incubated for 15 minutes at 37°C. The trypsin was neutralized with an equal volume of DMEM containing 10% FBS and antiobiotic/antimycotic (complete DMEM) and spun down for 5 minutes. The supernatant was aspirated and the cells were suspended in complete DMEM (10 mL) and seeded onto 10 cm dishes. The cells were then passaged 3T9 (every three days the cells were split 1:3 at a density of 900,000 cells per plate) to immortalize the cells. As the cells began to immortalize and slow down proliferation, we proceeded to a 3T6 passaging cycle.

Immunohistochemistry: Freshly harvested tissue was fixed in 4% paraformaldehyde for 48 hours, paraffin embedded, cut into 5 µm sections, and stained using an automated cell-stainer (Leica). Antibodies used for staining include those stated above and Ki-67 (Catalog # ab16667, Abcam). Ki67 stains were imaged using the Vectra multispectral microscope (PerkinElmer) and quantified using Informa software. In total, 10 ducts per mouse were quantified and averaged together using a batch analysis program before being compared between mice.

Results

Objective 1. *Determine if depletion of UbE2K, a negative regulator of PTEN leads to increases in PTEN protein levels and study its underlying mechanism.*

1.1 Knockdown of UbE2K in MCF10A cells led to a concomitant increase in PTEN protein levels, but not PTEN mRNA levels.

To assess whether depletion of the putative PTEN regulatory gene has any effect on PTEN *in vitro*, we transduced MCF10A cells, a normal mammary epithelial cell line, with lentivirus that coded for shRNAs targeting UbE2K. We assessed the efficiency of three shRNAs in HEK293t cells. Changes in mRNA levels of UbE2K were assessed by qRT-PCR with respect to the negative control sample, transfected with scrambled shRNA. We chose the shRNAs that most efficiently knocked down UbE2K and used it to deplete UbE2K from MCF10A cells. The UbE2K shRNA transduced MCF10A cells were then analyzed for changes in PTEN and UbE2K mRNA levels. Our data demonstrated an ~50% or 70% decrease in Ube2k mRNA levels, without any marked changes in PTEN mRNA levels. As expected, we observed a significant increase in PTEN protein levels in UbE2K depleted cells compared to the control (**Figure 6A**). A similar experiment was repeated in human patient-derived mammary fibroblasts, where we observed an increase in PTEN protein following depletion of UbE2K (**Figure 6B**). When treated with cycloheximide, a protein synthesis inhibitor, PTEN degradation was markedly delayed in the UbE2K depleted fibroblasts compared to that in the scramble shRNA (shNC) transduced fibroblasts (**Figure 6C**). These data suggest that knockdown of this negative regulator increased the stability of PTEN protein without significantly affecting PTEN mRNA levels in both mammary epithelial cells and fibroblasts.

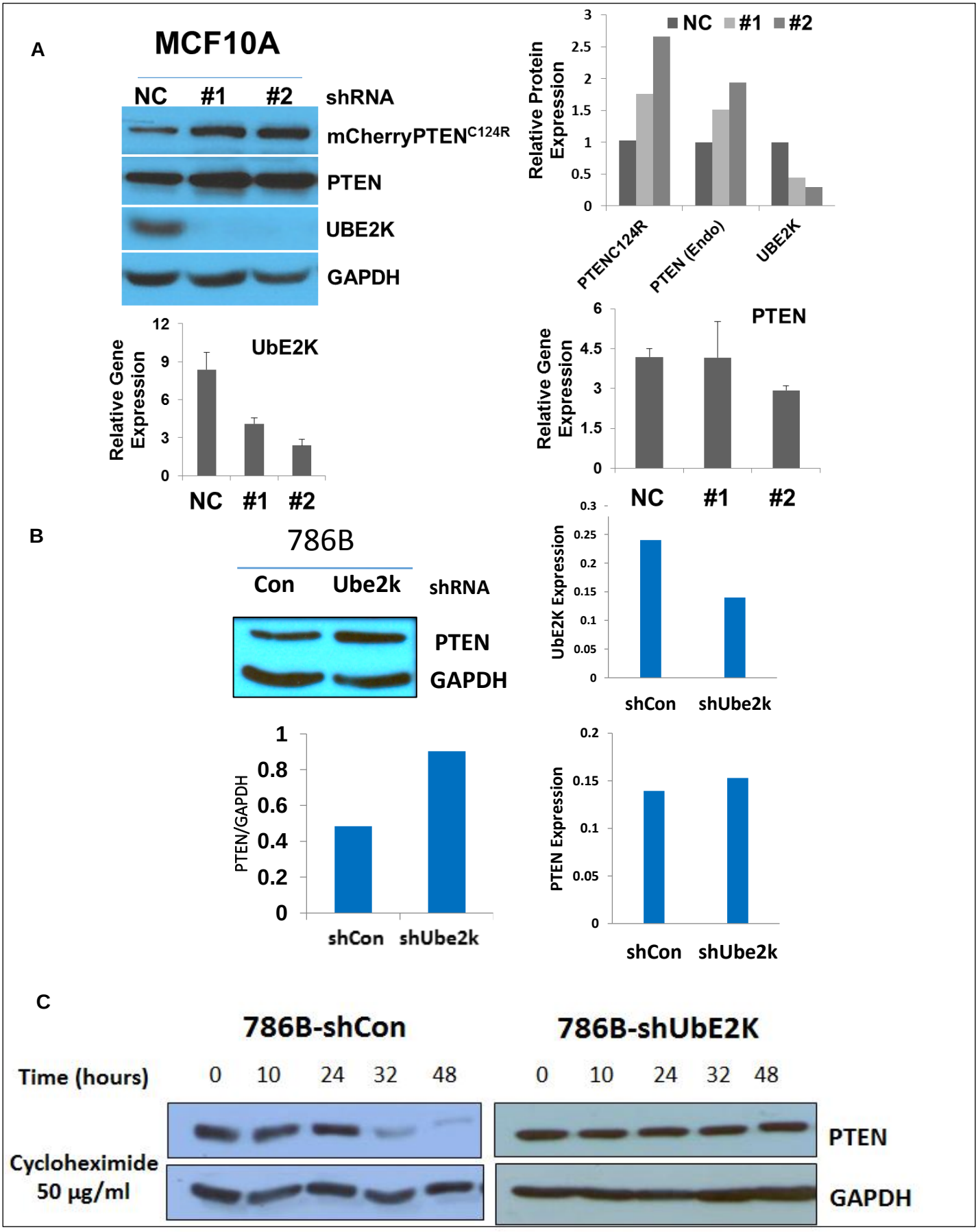

Figure 6 A) Knockdown of MCF10A cells using two non-overlapping shRNAs targeted towards UbE2K mRNA resulted in increased both PTEN^{C124R} and endogenous PTEN protein levels compared to a scrambled control. There were no significant changes in PTEN mRNA levels. B) Knockdown of UbE2K in patient-derived mammary fibroblasts recapitulated these results. C) Treatment of these fibroblasts with cycloheximide revealed an increase in PTEN stability upon depletion of UbE2K.

1.2 DNA damage induced Pten loss was rescued in Ube2k depleted cells

Wildtype Pten is a relatively stable protein. However, treatment of cells with DNA damaging agents like doxorubicin result in Pten destabilization [35]. We wanted to determine whether treatment of cells with agents like Doxorubicin would affect Pten levels in the control cells, but not in the *Ube2k* deleted cells. We generated cell lines genetically knocked out for *Ube2k* by isolating mouse embryonic fibroblasts (MEFs) at embryonic day 13.5 from an *Ube2k*$^{-/+}$ X *Ube2k*$^{-/+}$ breeding. Both wild-type (WT) and knockout (KO) lines for *Ube2k* were generated and immortalized through continuous passaging. We treated wild type (WT) and *Ube2k* KO MEFs, with 5 μM doxorubicin for 20 hours, and analyzed RNA and protein levels of Pten. We observed a marked decrease in the protein level in WT MEFs, but not in the *Ube2k* KO MEFs (**Figure 7B**). When we measured RNA levels between the treatment groups, we observed a decrease in *Pten* mRNA levels upon treatment with doxorubicin (**Figure 7C**). Despite this decrease in mRNA, Pten levels in the *Ube2k* KO MEFs appeared to be affected less than in the WT MEFs, suggesting that Pten levels were more stable upon Ube2k ablation with drug treatment.

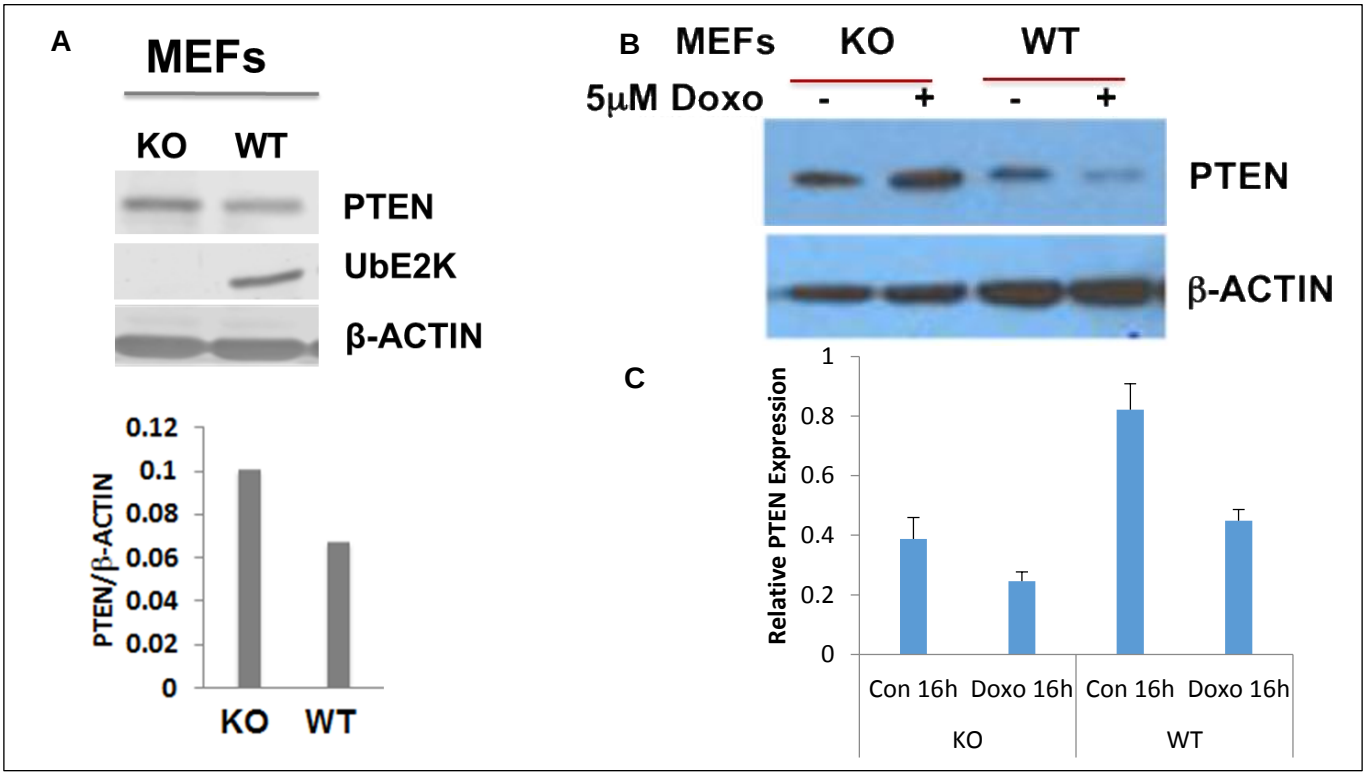

Figure 7 A) Ube2k KO MEFs display higher levels of Pten compared to control MEFs. B) Treatment of WT and Ube2k KO MEFs with the drug doxorubicin showed a stabilization of PTEN levels in the KO cells compared to the control. C) Treatment of MEFs with doxorubicin reduced Pten mRNA levels.

1.3 Loss of UbE2K increases PTEN levels in both the cytoplasmic and nuclear compartments

A defining characteristic of cancerous cells is loss of nuclear PTEN [36-41]. Nuclear PTEN plays a key role in chromosome stability, DNA repair, cell cycle arrest and cellular stability. Very little is known about PTEN protein turnover in the nuclear compartment. Thus, we wanted to know if the increase in PTEN protein we observed in *UbE2K* depleted cells was the result of stabilization of nuclear PTEN or if PTEN was stabilized in both the cytoplasm and nucleus. For this we fractionated MCF10A cells stably transduced with shUbE2k or scrambled shRNA, into cytoplasmic and nuclear compartments. We observed an increase in both cytoplasmic and nuclear PTEN in MCF10A cells upon UbE2K depletion compared to the scrambled shRNA transduced control cells. There was a more pronounced increase in the unstable $PTEN^{C124R}$ mutant compared to endogenous PTEN, as quantified in the bar diagram (**Figure 8**). From several iterations of similar experiments, we have found that changes in endogenous PTEN levels are difficult to detect due to the high stability of the protein.

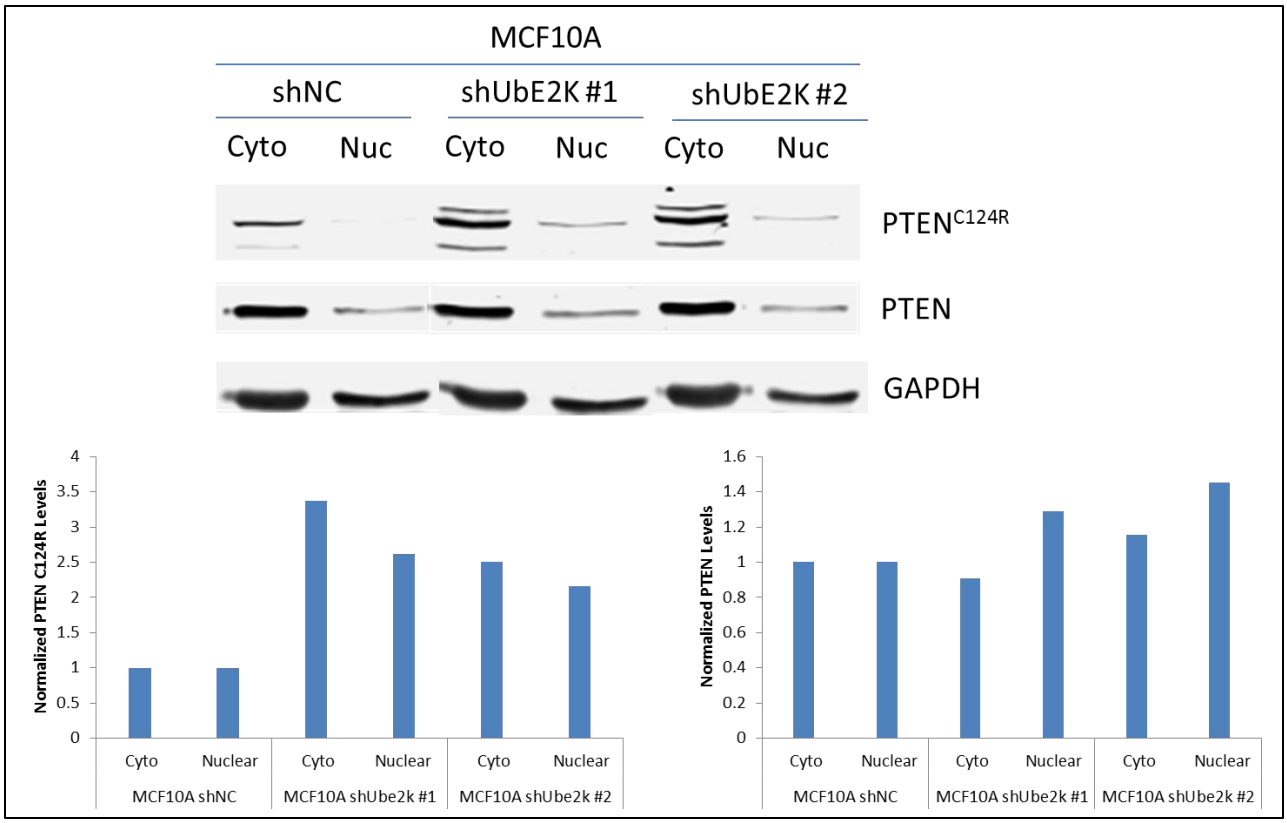

Figure 8 Targeted knockdown of UbE2K using two non-overlapping shRNAs in MCF10A cells followed by fractionation into cytoplasmic and nuclear compartments revealed an increase in both cytoplasmic and nuclear PTEN in the knockdown cells compared to a scrambled control.

1.4 Loss of UbE2K alters the ubiquitination profile of PTEN

UbE2K has been previously shown to specifically ubiquitinate substrates for proteasomal degradation. We next wanted to determine whether UbE2K mediates PTEN ubiquitination using Ube2k knockout MEFs. For this, we immunoprecipitated PTEN from WT and *Ube2k* KO MEFs. Following immunoprecipitation and immunoblotting with a PTEN-specific antibody, we noticed a dramatic difference in the profile of Pten in WT compared to KO cells, where high molecular weight Pten bands, presumably ubiquitinated, were lost in the KO cells (**Figure 9**). Further studies are being conducted to validate that these differences are due to ubiquitination rather than another post-translational modification. However, these results are promising because the only difference between these two MEF lines is the presence or absence of Ube2k, a mediator of proteasomal degradation.

.

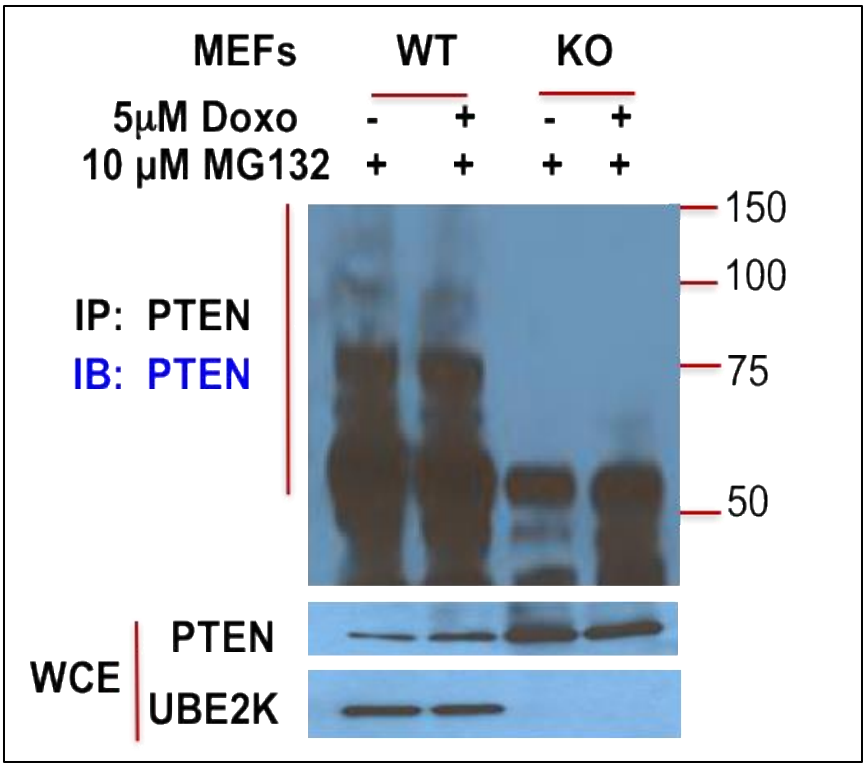

Figure 9 Immunoprecipitation of Pten from whole cell lysates of WT and Ube2k KO MEFs using a Pten antibody revealed differences in the Pten ubiquitination profile. These changes were maintained under Pten-destabilizing conditions by treatment with doxorubicin.

1.5 UbE2K may interact with the RNF5 E3 Ligase to promote PTEN degradation

In order to understand how the ubiquitin-proteasome pathway regulates PTEN levels, it is important to identify the E3 ligase(s) that partners with UbE2K to promote degradation of PTEN. While there are approximately 50 identified E2 conjugating enzymes, there are hundreds of identified E3 ligases. Thus, identifying the E3 ligases that complex with UbE2K to mediate the ubiquitination of PTEN is an important step in elucidating the entire pathway. A proteomics screen conducted in Dr. Michael Ostrowski's lab at The Ohio State University to identify PTEN interacting proteins revealed RNF5 as an E3 ligase that interacts with PTEN. Previous studies using a yeast-two hybrid system identified RNF5 as a binding partner of UbE2K, via the RING-domain in the E3 ligase [42]. Based on this information, we wanted to see whether RNF5 regulates PTEN protein stability similarly to UbE2K. We knocked down RNF5 in MCF10A cells using three different shRNAs and analyzed changes in mCherry-tagged-PTEN^{C124R} levels and endogenous PTEN levels. To further analyze our cell populations, we conducted FACS analysis to observe changes in mCherry intensity. Compared to parental and scrambled control lines, the cell lines infected with RNF5 shRNA showed an increase in mCherry intensity, confirming that there was an increase in PTEN^{C124R} levels in these cells (**Figure 10**). We then validated this increase in PTEN levels through western blotting and qPCR. We observed increases in both PTEN^{C124R} and endogenous PTEN protein along with a concomitant decrease in RNF5 levels. Similarly, we observed no significant changes in PTEN mRNA while there was a marked reduction in RNF5 mRNA levels (**Figure 11**). We are currently performing fractionation experiments on these RNF5 knockdown cells to see if we can recapitulate the increase in nuclear PTEN we observed upon knockdown of UbE2K. We also plan to repeat cycloheximide experiments in these cells to see if depletion of RNF5 renders PTEN more stable, similar to what we observed upon loss of UbE2K in fibroblasts.

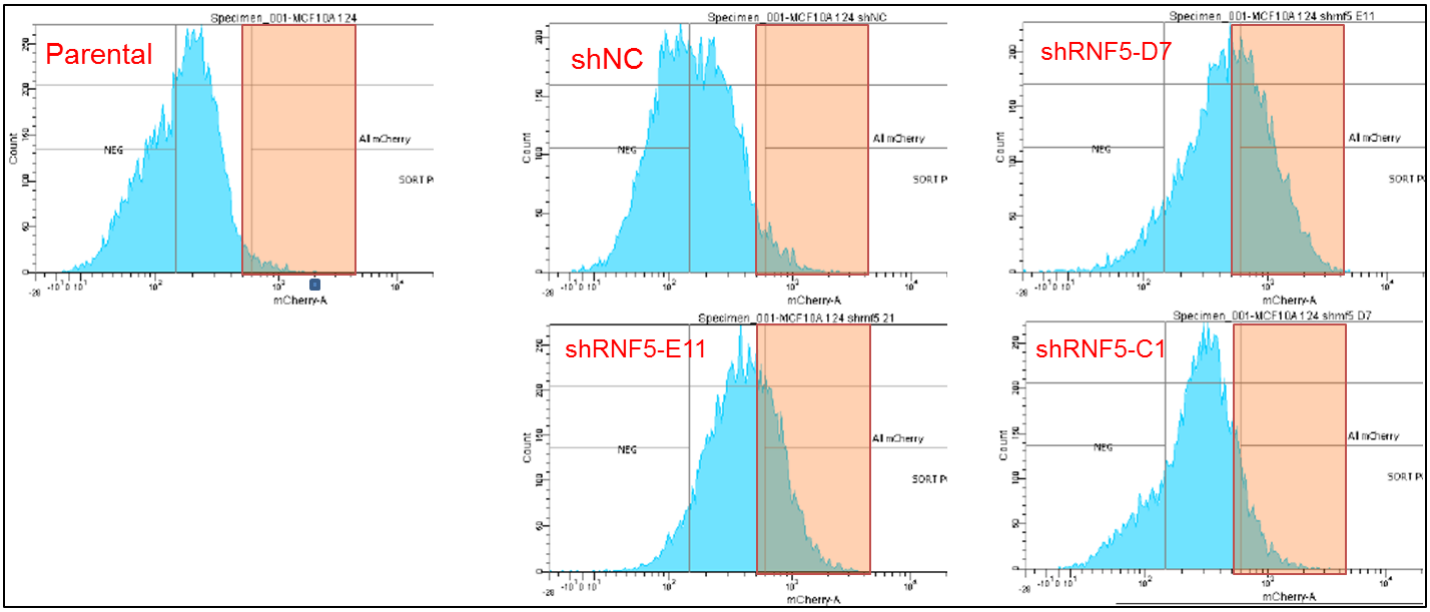

Figure 10 FACS analysis of MCF10A cells knocked down for RNF5 revealed an increase in mCherry intensity, correlating with an increase in PTEN^{C124R} levels compared to a scrambled control or parental lines.

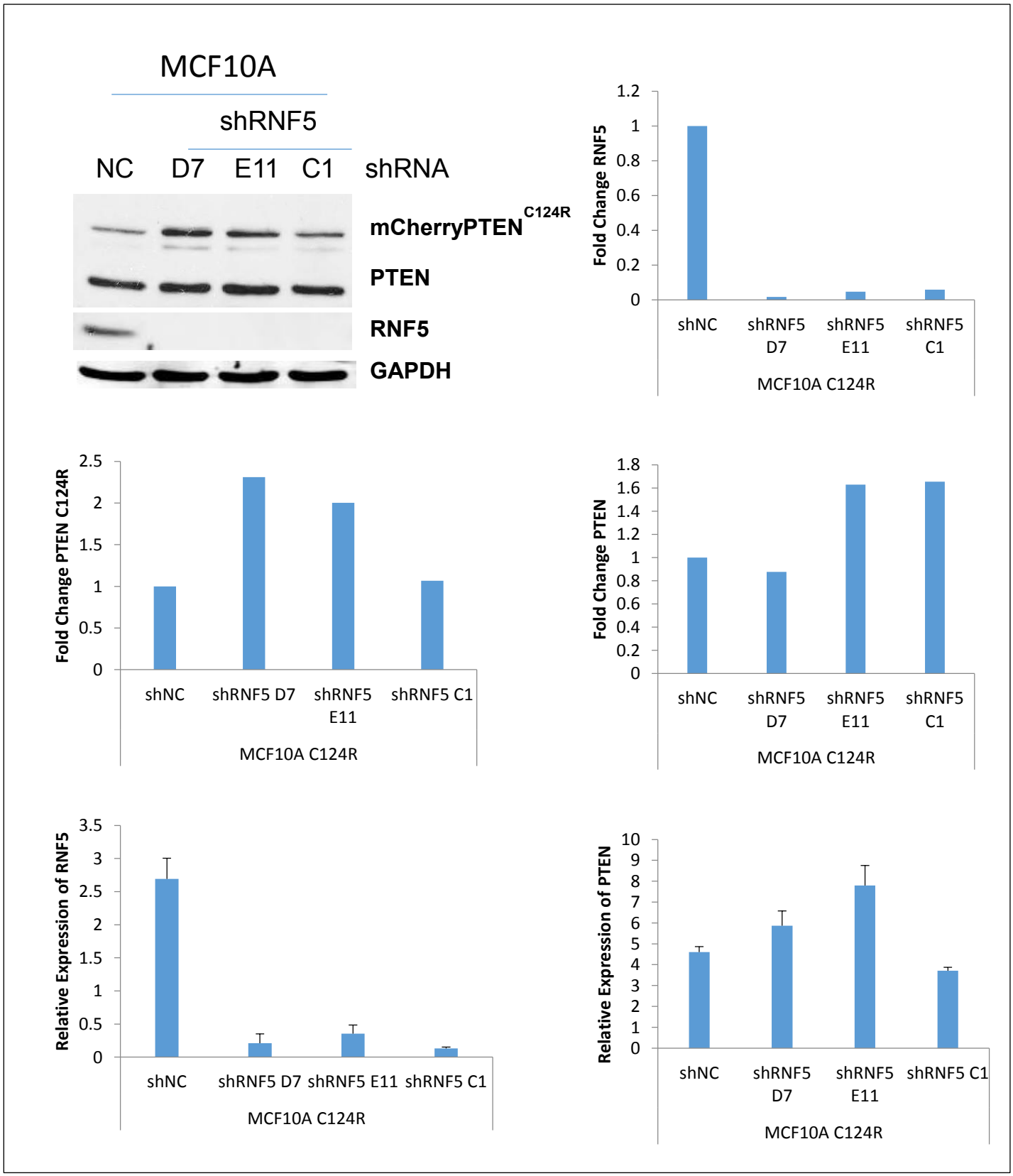

Figure 11 Depletion of RNF5 in MCF10A cells resulted in an increase in PTEN^{C124R} and endogenous PTEN protein levels. qRT-PCR showed a depletion in RNF5 mRNA, but no significant changes in PTEN mRNA.

Objective 2. *Study the effects of Ube2k deletion in the mammary epithelium and stromal fibroblasts in mice*

2.1 Ube2k neohypomorphs are viable and mimic the in vitro effect of Ube2k depletion

To understand the role of this putative regulator in a complex organism, we generated mice with conditional knockout alleles for *Ube2k* in the Leone lab, following IACUC guidelines (Protocol 2007A0239-R2). The targeting vector was obtained from KOMP (EUCOMM), where the Cre-Lox recombination system was used for targeted deletion of *Ube2k* (**Figure 12**). Briefly, mouse embryonic stem cells were electroporated with a vector containing an *Ube2k* allele with two loxP sites flanking exon 4 of the gene. The vector also contained a lacZ cassette and a neomycin resistance cassette flanked by FRT sites (see **Figure 12**, targeted allele). ES cells positive for the targeting vector were selected for using neomycin and were inserted into a pseudo-pregnant mouse, producing chimeric mice. When the allele became germline, these mice were bred with *ACTFLPe* mice to delete the lacZ and neo cassettes, producing heterozygous "floxed" mice which were used for further breedings.

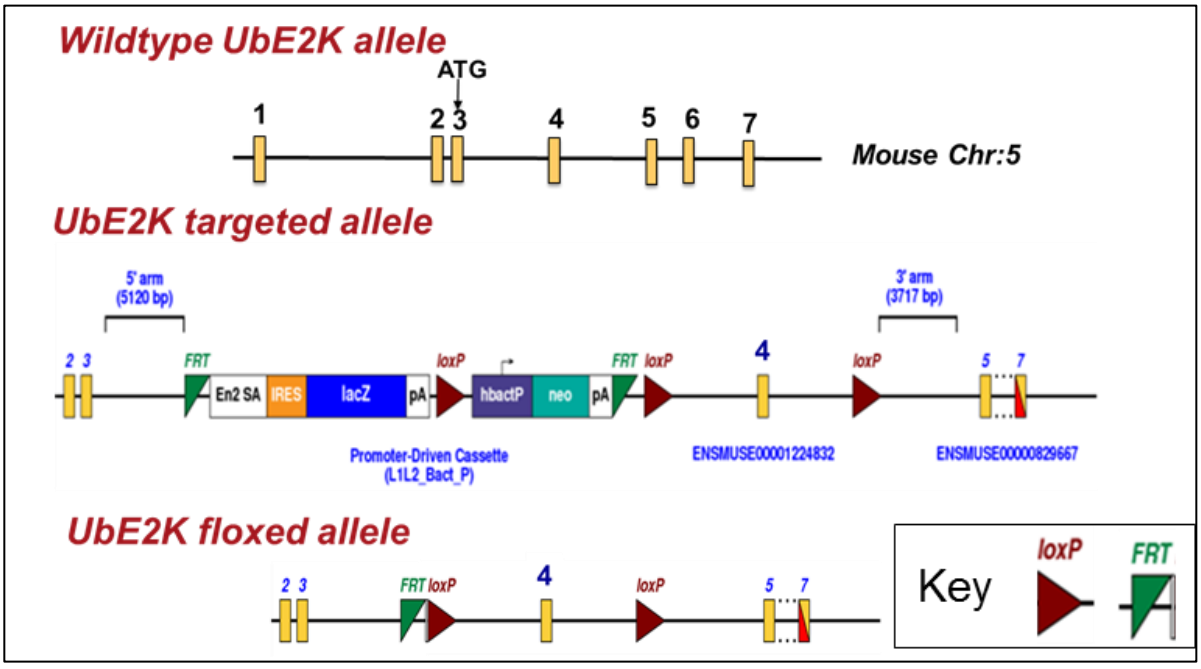

Figure 12 Targeting vector for the *Ube2k* allele. LoxP sites were introduced flanking exon 4 of the *Ube2k* gene and a LacZ-Neo Cassette was introduced between exons 3 and 4 flanked by FRT sites.

We first studied the cassetted Ube2k neohypomorph (*Ube2k*$^{neo/neo}$) mice. Immunohistochemical analysis of day 13.5 embryos revealed Ube2k to be absent in the neohypomorphs, whereas Pten levels were increased compared to WT littermates (**Figure 13**). These mice are viable and fertile; however, they are runted compared to their wild-type littermates (**Figure 14A**). We next harvested and analyzed different tissues from 60 day old male and female neohypomorphs. Analysis of the liver sections revealed predominantly nuclear localization of Ube2k in the hepatocytes of the WT mice, which is completely lost in the neohypomorphs. A striking increase in nuclear localization of Pten was observed in the neohypomorphs, demonstrating a reciprocal relationship between the two proteins *in vivo* (**Figure 14B, C**). This finding also corroborates our *in vitro* data where we observed an increase in nuclear PTEN after depletion of UbE2K using shRNAs.

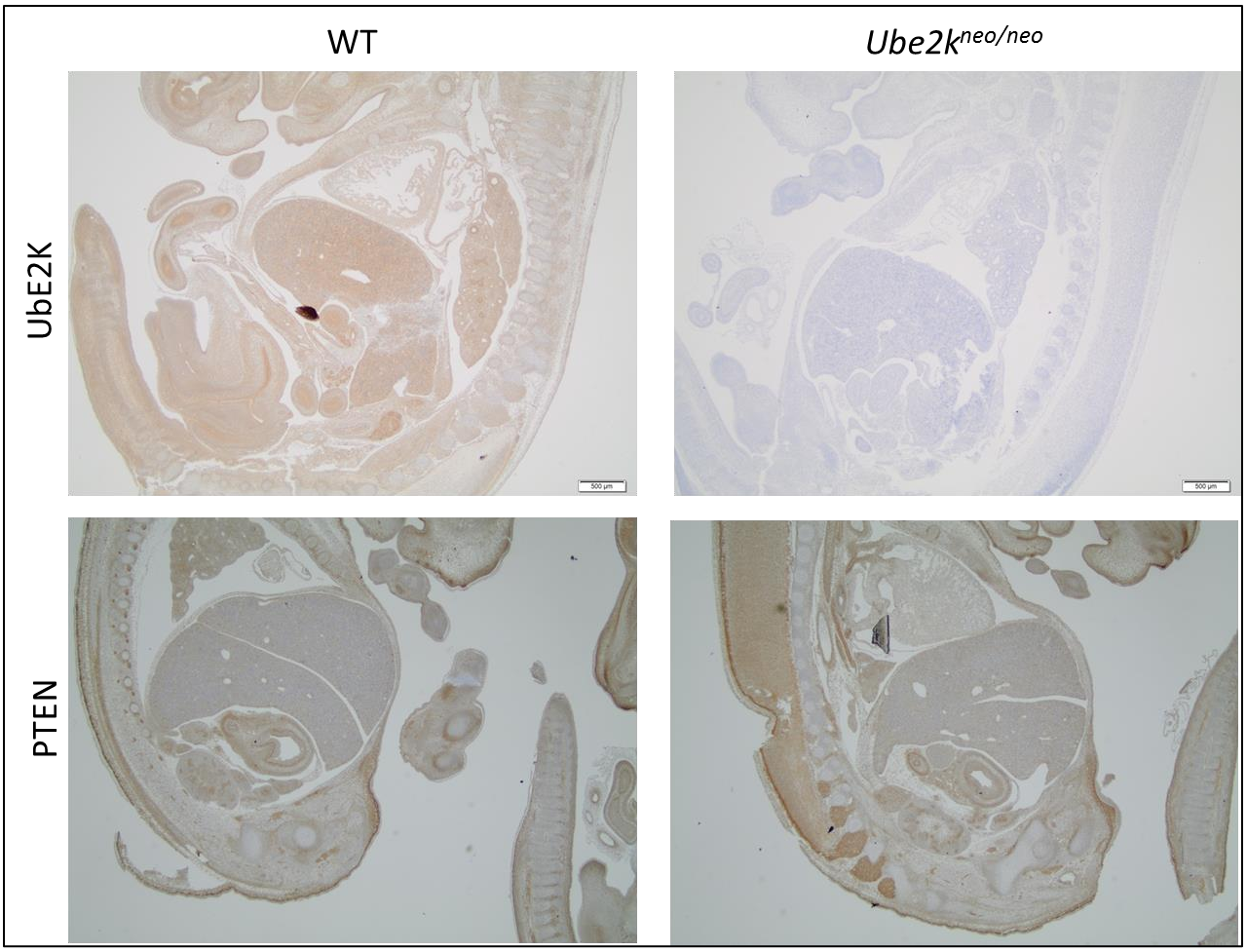

Figure 13 Immunohistochemical analysis of E13.5 embryos revealed a loss of Ube2k and a concomitant increase in Pten levels.

We have also harvested mammary glands from two month old female mice and performed dual-immunofluorescence on the mammary gland to study the relationship between Pten and Ube2k levels. We found that Ube2k (in red) is highly expressed in the nuclei of the mammary epithelial cells of the wildtype mice, and is significantly reduced in the neohypomorphs. Analysis of Pten (in green) levels demonstrated markedly higher levels of nuclear Pten in the mammary epithelium of the neohypomorph compared to that in the wild-type littermates (**Figure 15**). We also observed this reciprocal relationship in areas of the stroma where Ube2k is expressed. This observation further supports our hypothesis that Ube2k is a negative regulator of Pten in the mammary epithelium and stroma and corroborates our *in vitro* data.

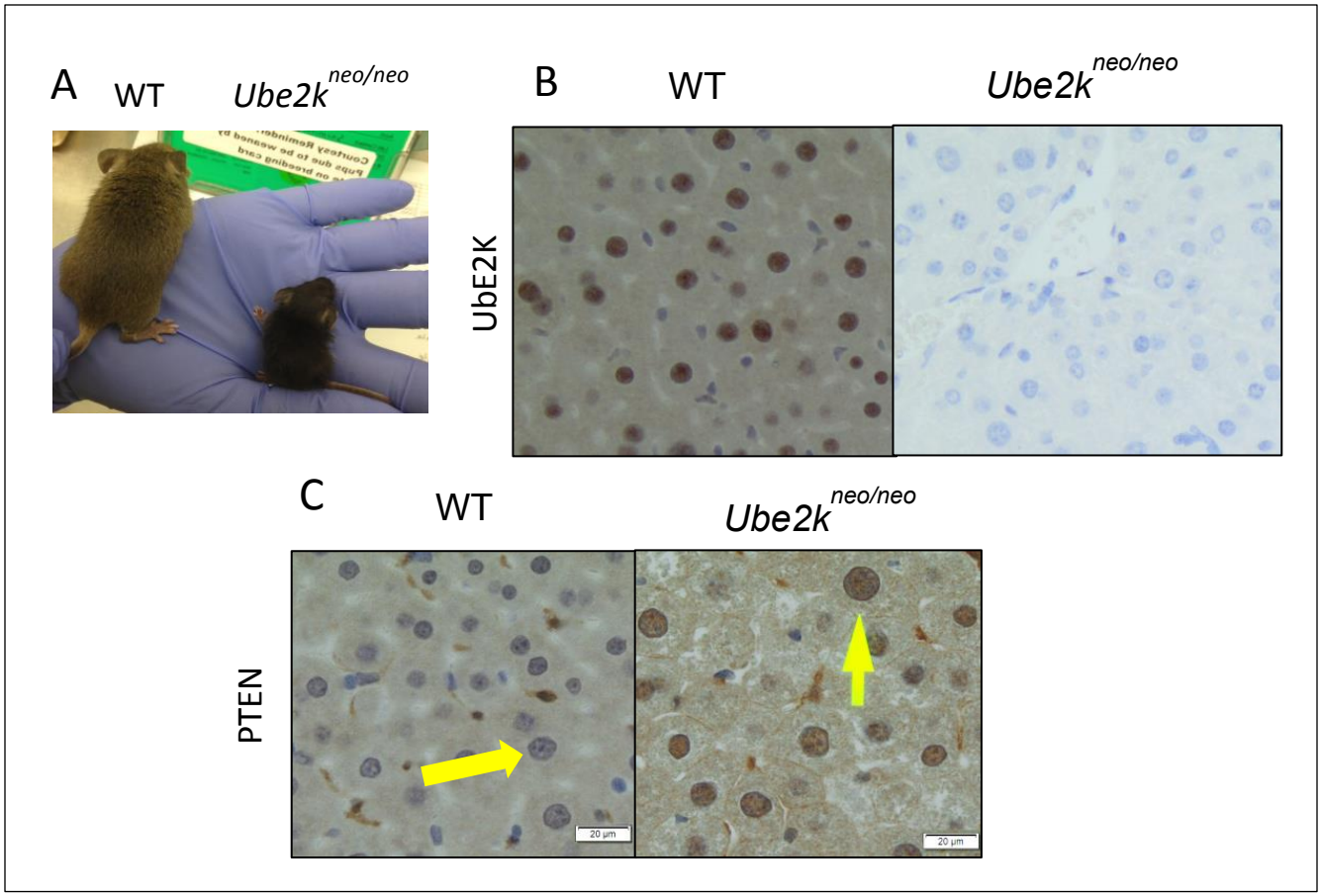

Figure 14 A) Disruption of Ube2k results in a runted developmental phenotype B) Ube2k shows primarily nuclear localization in WT mice which is lost in the neohypomorphs C) loss of Ube2k resulted in nuclear localization of PTEN in the hepatocytes of 60 day old mice.

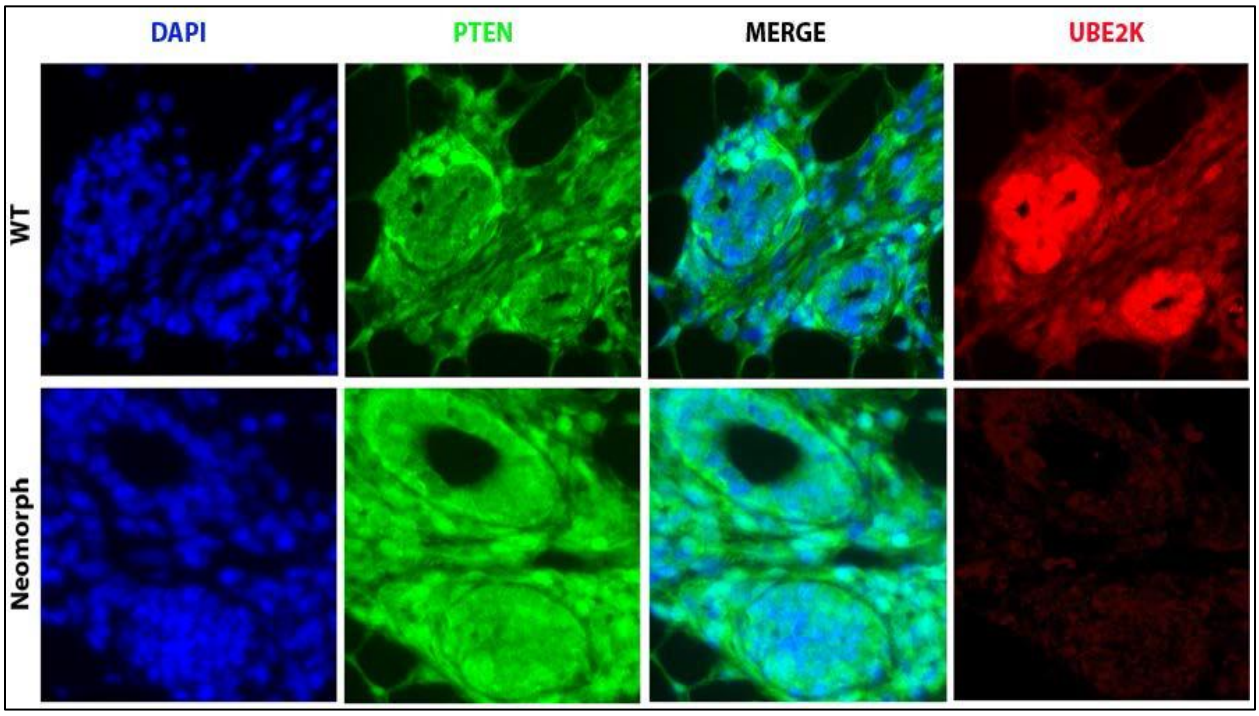

Figure 15 Dual-immunofluorescence analysis of 2 month old WT and neomorph mammary glands revealed an inverse relationship between Ube2k and Pten protein levels (note the loss of nuclear Pten in the mammary epithelium in the WT mice where Ube2k is expressed strongly).

2.2 Mice with conditional knockout alleles for Ube2k recapitulated our in vitro results and produced phenotypic abnormalities.

To delete the l*acZ-neo* artificial cassette, we bred *Ube2k*$^{neo/neo}$ *mice* (targeted allele, **Figure 12**) with *ACTFLPe* mice and obtained mice with an Ube2k floxed allele (Ube2k$^{fl/fl}$). We then generated whole body knockout mice (KO) for *Ube2k* by breeding the Ube2k$^{fl/fl}$ mice with Sox2-Cre mice. Genotyping was conducted using a three-primer PCR system that recognized the WT, floxed, and knockout alleles represented by 370 bp, 447 bp and 617 bp PCR products as shown in **Figure 16**. We have noted that the *Ube2k* KO mice have severe developmental defects compared to the neohypomorphs (**Figure 17A**). Most KO pups die within two days of birth and weigh less than littermate WT and heterozygous (Het) pups (**Figure 17B**). Ube2k KO mice appear to be born at numbers lower than the predicted Mendelian ratio. We have harvested tissues from P2 (post natal day 2) pups and stained them with Haematoxylin and Eosin (H&E) to assess any histological changes. We have also determined the status of Ube2k and Pten protein levels by IHC to assess any changes in Pten levels and to see

whether or not we can recapitulate our *in vitro* data where we observed a reciprocal relationship between Pen and Ube2k levels. These analyses are currently being conducted.

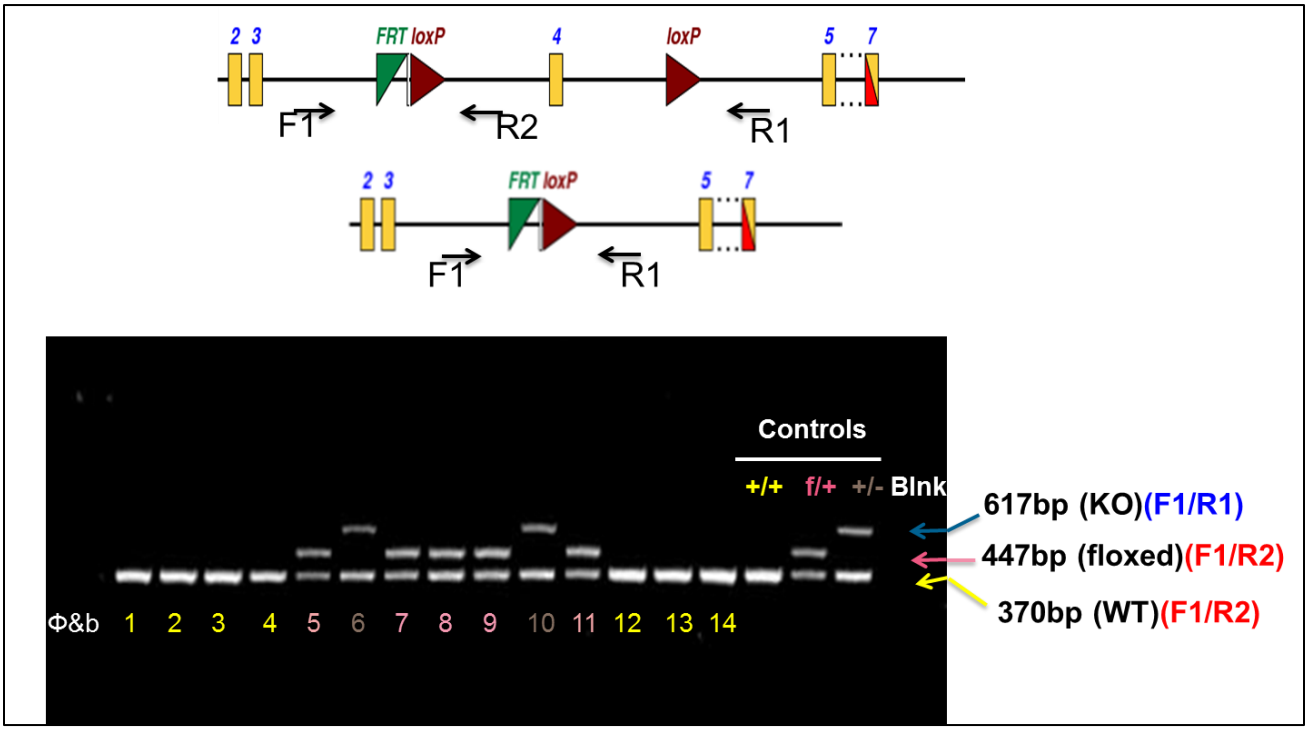

Figure 16 Schematic used for genotyping *Ube2k* conditional mice along with a representative gel showing the banding pattern for all three potential PCR products.

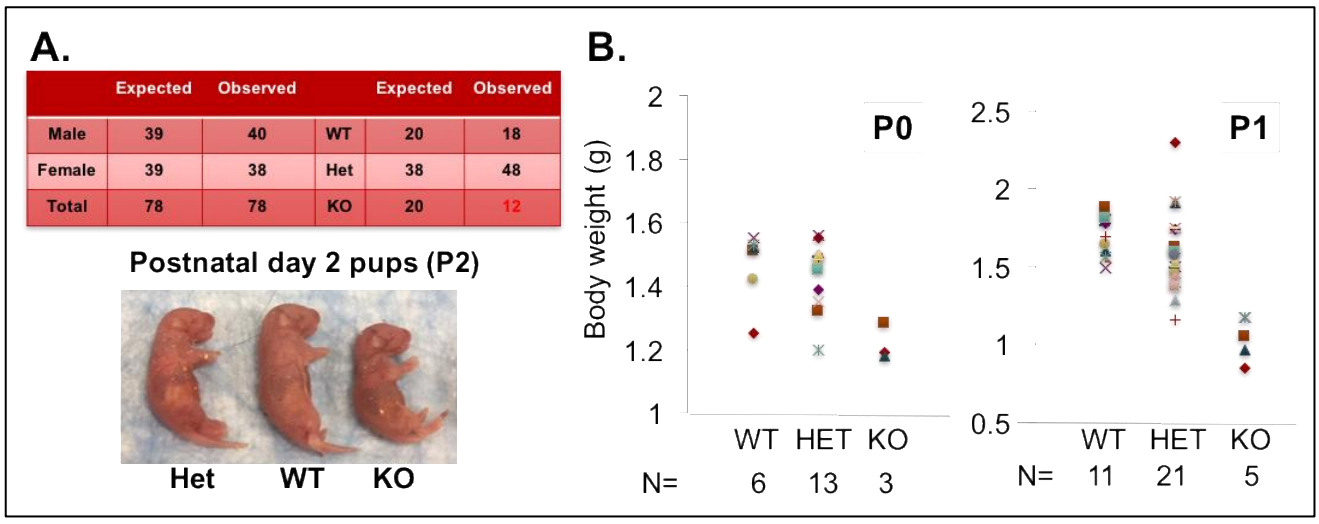

Figure 17 A) Whole-body Ube2k KO pups are runted at after birth compared to WT and heterozygous (Het) littermates and typically die within two days of birth. B) Ube2k KO pups weigh less than WT or Het littermates.

2.3 Loss of Ube2k in the stromal fibroblasts leads to decreased branching in the mammary gland

Because whole body knockout of *Ube2k* resulted in early post-natal lethality, we generated conditional knockout mice by deleting *Ube2k* specifically in the stromal fibroblasts using *Fsp-cre.* For this we bred mice harboring conditional alleles for *Ube2k* with mice expressing the stroma-specific recombinase, Fsp-Cre. We aged the experimental (*Fsp-Cre; Ube2k*$^{fl/fl}$) and control (*Ube2k*$^{fl/fl}$) littermates to three months of age, when mammary gland development has completed. The mammary gland undergoes dynamic changes throughout the adult life of the females due to hormonal changes that occur as a result of the estrus cycle [43]. Thus, it is important to ensure that all mice were harvested at the same stage of the estrus cycle. We chose to harvest the experimental and control mice at diestrus because this is the most proliferative phase for the mammary gland. We hypothesized that this will amplify any differences in proliferation resulting from the presence or absence of stromal UbE2K that in turn is expected to reciprocally regulate Pten levels. We observed decreased branching in the experimental mice when compared with an age-matched control. Immunohistochemistry for Pten and Ube2k performed on consecutive sections showed that *Ube2k* deletion was specific to the stromal fibroblasts and that Pten levels increased in both the epithelium and stroma (**Figure 18**). We are currently performing experiments to determine whether this difference arises from increased levels of Pten, which would suppress cell proliferation, or from an off target effect of *Ube2k* deletion in the stromal fibroblasts.

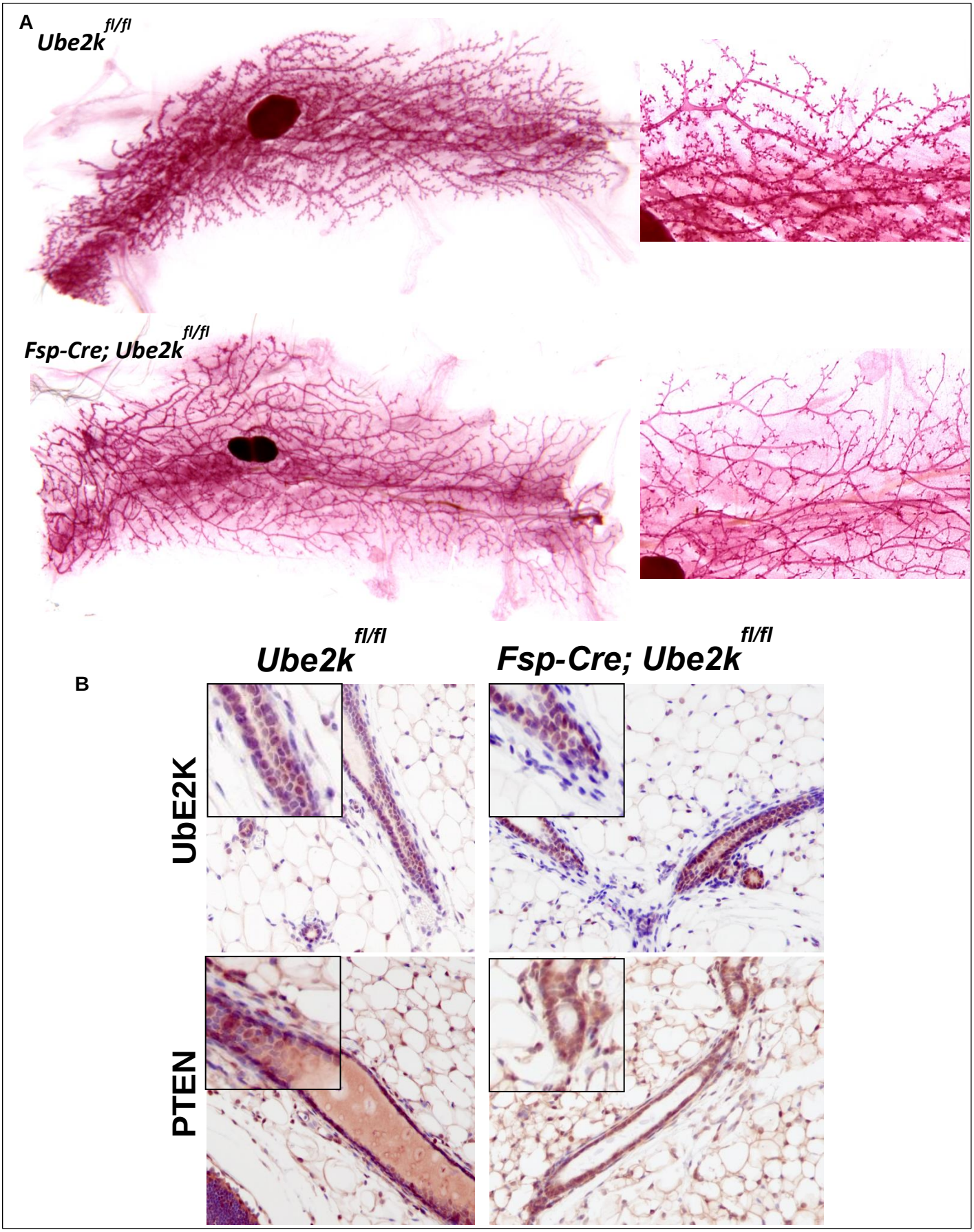

Figure 18 A) Whole mounts of mammary glands from 12 week old mice at diestrus and stained with Carmine red revealed a decrease in alveologenesis upon deletion of *Ube2k* in stromal fibroblasts. B) UBE2K IHC demonstrates fibroblast-specific deletion of Ube2k and shows a concomitant increase in Pten levels in both the epithelium and stroma.

2.4 Loss of Ube2k in the stromal fibroblasts of the mammary gland results in decreased proliferation of mammary epithelial cells.

After observing a difference in the branching pattern of the mammary gland in mice with a stromal deletion of Ube2k, we performed IHC on mammary gland sections from the same mice to determine whether markers of cell proliferation were altered in the experimental group. After staining the sections for Ki67, a cell proliferation marker, we observed a significant reduction of Ki67 positive cells in the Ube2k-deleted mice compared to that in the controls (**Figure 19**). This decrease in proliferation explains the reduced branching phenotype we observed and supports our hypothesis that reduction of Ube2k leads to an increase in Pten in the fibroblasts, and cross-talk between the altered stroma and epithelium might have led to suppression of cell proliferation. Additional studies are in progress to validate if altered Pten levels are the key mediator of epithelial proliferation.

These findings were tested using an *in vitro* co-culture model in parallel. Breast cancer cell lines with a DsRed reporter were cultured in matrigel with patient-derived fibroblasts expressing either basal levels of UbE2K or depleted UbE2K using shRNA. The proliferation rate of the epithelial cells was markedly decreased when co-cultured with fibroblasts containing reduced levels of UbE2K compared to control fibroblasts (**Figure 20**). These data suggest that depletion of stromal UbE2K can affect the proliferation rate of the epithelium. We have yet to establish that this effect is dependent on PTEN levels, but our *in vitro* data suggests that this could be the mechanism involved. We also plan to study the mechanism of how loss of stromal UbE2K affects proliferation in the epithelium. Identifying this signaling mechanism will offer important insight into how these two compartments cross-talk in normal and cancerous cells.

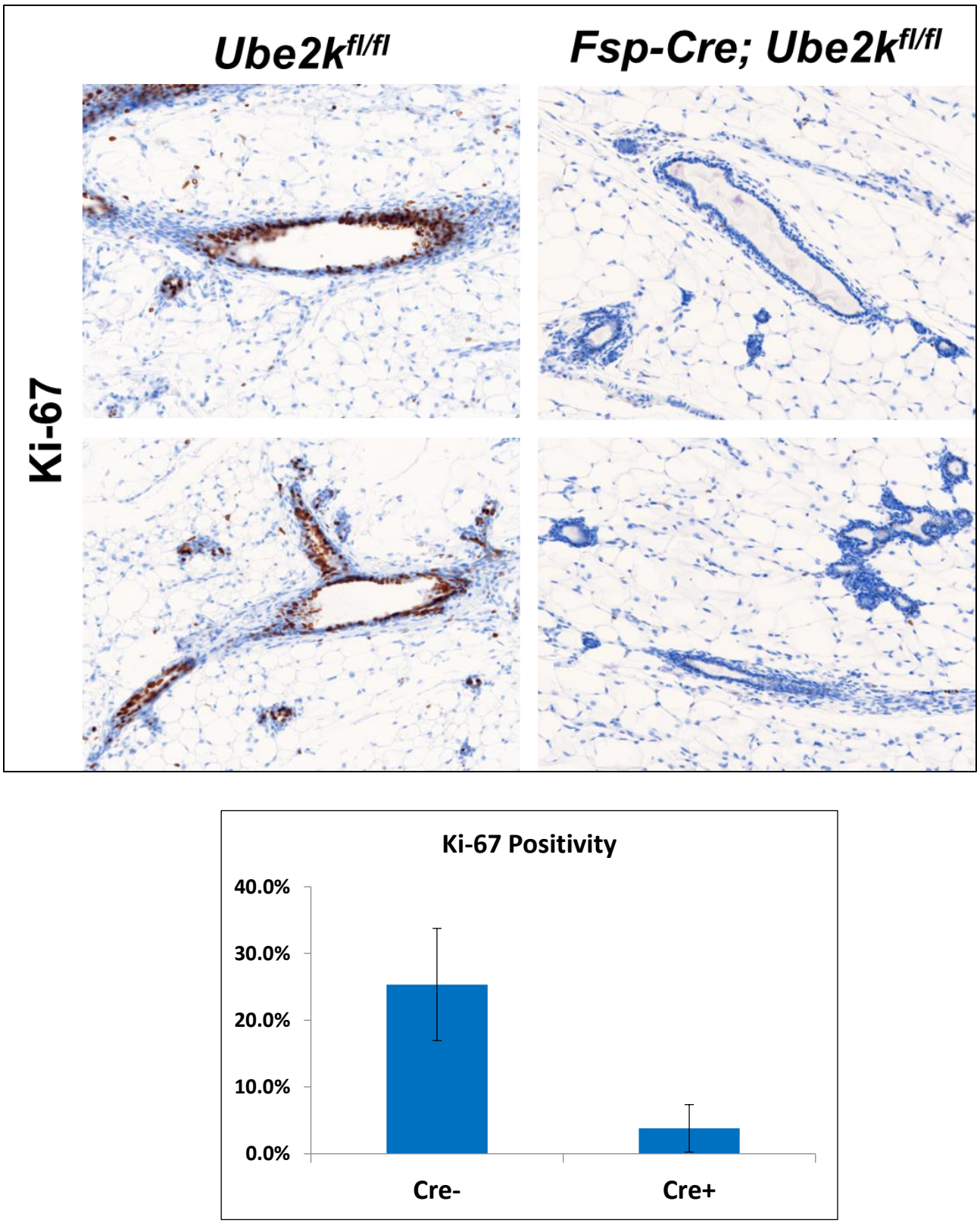

Figure 19 Ki-67 IHC of 12 week mammary gland in diestrus confirmed that epithelial proliferation in the control mice was markedly higher than in the mice with loss of stromal Ube2k.

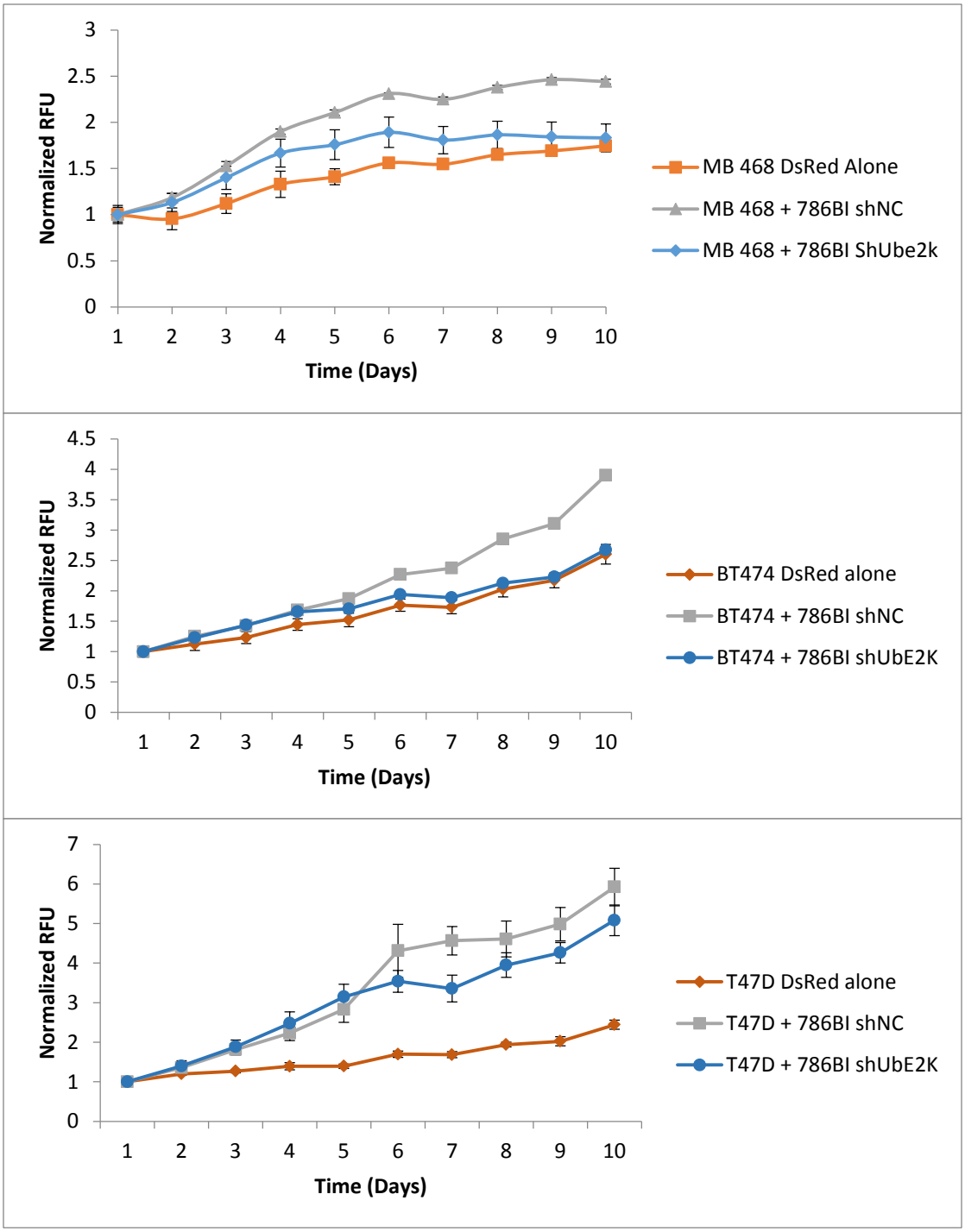

Figure 20 Co-culture of DsRed tagged epithelial cells with patient-derived fibroblasts revealed a decrease in proliferation upon loss of UbE2K in the fibroblasts.

Discussion

Our concerted effort to identify factors regulating PTEN protein stability has led to the identification of an E2 conjugating enzyme, UBE2K, and alludes to a role of the ubiquitin-proteasome pathway in PTEN degradation. We observed a reciprocal relationship between UbE2K and PTEN levels in cells, suggesting that UbE2K negatively regulates PTEN. These results were validated in both *in vitro* and *in vivo* models. These findings could be important clinically, as low PTEN levels correlate with poor disease outcome in almost all cancers, including triple negative breast cancer. Furthermore, post-translational modifications that compromise the normal function of PTEN could potentially explain how individuals without a genetic mutation in *PTEN* could become predisposed to develop cancer.

In vitro knockdown of UbE2K using non-overlapping shRNAs in MCF10A cells resulted in an increase in PTEN protein independent of its mRNA level. Furthermore, UbE2K depletion resulted in an increase in the amount of nuclear PTEN. It is important to note that Ube2k is predominantly localized in the nucleus, particularly in the hepatocytes and mammary epithelium. Nuclear PTEN has been implicated in maintaining genomic stability, which is frequently compromised in cancer cells. Our finding suggests that Ube2k could be involved in Pten turnover in the nucleus and thus stabilization of PTEN by targeting UbE2K could be beneficial for cancer patients. However, it is important to conduct additional studies to suggest this possibility, as UbE2K is expected to have several other targets. We hypothesize that nuclear PTEN is degraded in the presence of UbE2K. Because UbE2K is specific for proteasomal degradation and not translocation like some other E2 enzymes, it is likely that blocking degradation accounts for the increase in nuclear PTEN and not a failure to export PTEN from the nucleus. It has already been shown that monoubiquitination of PTEN at Lys13 and Lys289 regulates shuttling between the cytoplasmic and nuclear compartments [39]. Meanwhile, polyubiquitination at Lys289 by molecules like NEDD4 and MKRN1 have been shown to target PTEN for proteasomal degradation. Thus, it will be important to map the Lys residues targeted by PTEN by its potential binding partner RNF5 to gain important insight into how these genes regulate PTEN levels.

We have also observed alteration in the Pten ubiquitination profile in Ube2k KO MEFs, suggesting that Ube2k mediates the ubiquitination of Pten. A second proteomics study conducted in our group to identify PTEN interacting proteins has identified RNF5, a Ring Finger E3 ligase, as a potential E3 ligase that binds to PTEN. Previous studies using a yeast-two hybrid assay system have shown RNF5 is a binding partner of UbE2K [42]. Based on this information we have depleted RNF5 in MCF10A cells, and observed a similar increase in PTEN levels, supporting our hypothesis that UbE2K and RNF5 might work in concert to regulate PTEN degradation. Interestingly, previous studies have shown that increased RNF5 levels correlate with poor disease outcome in breast cancer patients [44]. We are currently performing additional studies to validate these observations and determine whether overexpression or knockdown of RNF5 alters the ubiquitination profile of PTEN similar to UbE2K. More long-term experiments consist of generating conditional and whole-body knockout mice for Rnf5 and generating MEFs to study the role of Rnf5 both *in vitro* and *in vivo*—similar to those performed with Ube2k KO mice and MEFs. Several other E3 ligases for PTEN have also been reported in the literature, including NEDD4, MKRN1, and WWP2 that could be revisited in the context of UbE2K.

In general, our *in vivo* experiments in mice recapitulated our *in vitro* observations. We observed negative staining of Ube2k by IHC in both whole-body and conditional knockout mice with a concomitant increase in Pten. Loss of stromal Ube2k in the mammary gland had an effect on Pten levels in the epithelium and suppressed proliferation. While these results are promising and corroborate our hypothesis, we still need to demonstrate that Ube2k deletion and subsequent Pten protein stabilization in the stromal fibroblasts is the key determinant of the reduced proliferation rate of the mammary epithelium in these mice. It will be important to determine whether these changes in Pten levels in the stromal fibroblasts are able to suppress proliferation of mammary tumor cells. We plan to use the ErbB2-neu tumor model similar to the one used in *Trimboli et al.* in an FVB/N background to see whether increasing Pten levels via deletion of Ube2k in the stroma alters the progression of the tumors. Based on our hypothesis, we predict that increasing Pten levels will slow down or inhibit the

growth of these tumors, as researchers have previously shown that stromal Pten suppresses mammary epithelial tumors.

Our studies aim to elucidate the pathways responsible for PTEN turnover in cells, as this area remains relatively unexplored and may provide insight into PTEN pathophysiology. Identifying these enzymes could provide novel targets for treatment using therapeutics such as proteasome inhibitors or targeted siRNA delivery. Furthermore, because PTEN is one of the most frequently lost tumor suppressors in human cancer, our findings may potentially translate into other cancers such as endometrial, pancreatic, prostate, thyroid, and others.

References

1. Network, C.G.A., *Comprehensive molecular portraits of human breast tumours.* Nature, 2012. 490(7418): p. 61-70.
2. Trimboli AJ, Cantemir-Stone CZ, Li F, et al. Pten in stromal fibroblasts suppresses mammary epithelial tumours. Nature. 2009;461(7267):1084-1091.
3. Li, J. *et al.* PTEN, a putative protein tyrosine phosphatase gene mutated in human brain, breast, and prostate cancer. *Science* 275, 1943–1947 (1997).
4. Steck, P. A. *et al.* Identification of a candidate tumour suppressor gene, *MMAC1*, at chromosome 10q23.3 that is mutated in multiple advanced cancers. *Nature Genet.* 15, 356–362 (1997).
5. *Shi Y, Wang J, Chandarlapaty S, Cross J, Thompson C, Rosen N, Jiang X (Jun 2014). "PTEN is a protein tyrosine phosphatase for IRS1". Nature Structural & Molecular Biology 21 (6): 522–7.*
6. *Shnitsar I, Bashkurov M, Masson GR, Ogunjimi AA, Mosessian S, Cabeza EA, Hirsch CL, Trcka D, Gish G, Jiao J, Wu H, Winklbauer R, Williams RL, Pelletier L, Wrana JL, Barrios-Rodiles M (2015-09-24). "PTEN regulates cilia through Dishevelled". Nature Communications 6: 8388.*
7. Song MS, Salmena L, Pandolfi PP. The functions and regulation of the PTEN tumour suppressor. Nat Rev Mol Cell Biol. 2012;13(5):283-296.
8. Di Cristofano, A., Kotsi, P., Peng, Y.F., Cordon-Cardo, C., Elkon, K.B., and Pandolfi, P.P. (1999). Impaired Fas response and autoimmunity in Pten+/− mice. Science 285, 2122–2125.
9. Hollander MC, Blumenthal GM, Dennis PA. PTEN loss in the continuum of common cancers, rare syndromes and mouse models. *Nat Rev Cancer*. 2011;11(4):289-301.
10. Wang H, Karikomi M, Naidu S, et al. Allele-specific tumor spectrum in PTEN knockin mice. *Proc Natl Acad Sci U S A*. 2010;107(11):5142-5147.
11. Wallace JA, Li F, Leone G, Ostrowski MC. Pten in the breast tumor microenvironment: Modeling tumor-stroma coevolution. *Cancer Res*. 2011;71(4):1203-1207.
12. Shi Y, Paluch BE, Wang X, Jiang X. PTEN at a glance. *J Cell Sci*. 2012;125(Pt 20):4687-4692.
13. Jang HD, Noh JY, Shin JH, Lin JJ, Lee SY. PTEN regulation by the Akt/GSK-3β axis during RANKL signaling. *Bone*. 2013;55(1):126–131
14. Huang J, Yan J, Zhang J, et al. SUMO1 modification of PTEN regulates tumorigenesis by controlling its association with the plasma membrane. *Nat Commun*. 2012;3:911.
15. Okumura K, Mendoza M, Bachoo RM, DePinho RA, Cavenee WK, Furnari FB. PCAF modulates PTEN activity. *J Biol Chem*. 2006;281(36):26562–26568.
16. Wang X, Trotman LC, Koppie T, et al. NEDD4-1 is a proto-oncogenic ubiquitin ligase for PTEN. *Cell*. 2007;128(1):129-139.
17. Lee MS, Jeong MH, Lee HW, et al. PI3K/AKT activation induces PTEN ubiquitination and destabilization accelerating tumourigenesis. *Nat Commun*. 2015;6:7769.
18. Manning, B.D., and Cantley, L.C. (2007). AKT/PKB signaling: navigating downstream. Cell *129*, 1261–1274.
19. Maira SM, Pecchi S, Huang A, Burger M, Knapp M, Sterker D, et al. Identification and characterization of NVP-BKM120, an orally available pan-class I PI3-kinase inhibitor. Mol Cancer Ther 2012;11:317-328.
20. Lee JJ, Loh K, Yap YS. PI3K/Akt/mTOR inhibitors in breast cancer. *Cancer Biol Med*. 2015;12(4):342-354.
21. Ye Y, Rape M. Building ubiquitin chains: E2 enzymes at work. *Nat Rev Mol Cell Biol*. 2009;10(11):755-764.
22. Pickart, C. M. & Fushman, D. Polyubiquitin chains: polymeric protein signals. *Curr. Opin. Chem. Biol.* **8**, 610–616 (2004).
23. Kerscher, O., Felberbaum, R. & Hochstrasser, M. Modification of proteins by ubiquitin and ubiquitin-like proteins. *Annu. Rev. Cell Dev. Biol.* **22**, 159–180 (2006).
24. Song, S. *et al.* Essential role of E2-25K/Hip-2 in mediating amyloid-beta neurotoxicity. *Mol. Cell* **12,** 553–563 (2003).

25. Chen, Z. & Pickart, C. M. A 25-kilodalton ubiquitin carrier protein (E2) catalyzes multi-ubiquitin chain synthesis via lysine 48 of ubiquitin. *J. Biol. Chem.* **265,** 21835–21842 (1990).
26. Rodrigo-Brenni, M.C. and D.O. Morgan, *Sequential E2s drive polyubiquitin chain assembly on APC targets.* Cell, 2007. 130(1): p. 127-39.
27. Christensen, D.E., P.S. Brzovic, and R.E. Klevit, *E2-BRCA1 RING interactions dictate synthesis of mono- or specific polyubiquitin chain linkages.* Nat Struct Mol Biol, 2007. 14(10): p. 941-8.
28. Brandman O, Stewart-Ornstein J, Wong D, Larson A, Williams CC, Li GW, Zhou S, King D, Shen PS, Weibezahn J, Dunn JG, Rouskin S, Inada T, Frost A, Weissman JS. A ribosome-bound quality control complex triggers degradation of nascent peptides and signals translation stress. Cell. 2012; 151:1042–1054.
29. Defenouillere Q, Yao Y, Mouaikel J, Namane A, Galopier A, Decourty L, Doyen A, Malabat C, Saveanu C, Jacquier A, Fromont-Racine M. Cdc48-associated complex bound to 60S particles is required for the clearance of aberrant translation products. Proceedings of the National Academy of Sciences of the United States of America. 2013; 110:5046–5051.
30. Verma R, Oania RS, Kolawa NJ, Deshaies RJ. Cdc48/p97 promotes degradation of aberrant nascent polypeptides bound to the ribosome. eLife. 2013; 2:e00308.
31. Delcros JG, Floc'h MB, Prigent C, Arlot-Bonnemains Y. Proteasome inhibitors as therapeutic agents: current and future strategies. Current medicinal chemistry. 2003; 10:479–503.
32. Röllig C, Knop S, Bornhäuser M. Multiple myeloma. Lancet. 2014; Dec :pii. S0140-673660493-1
33. Izumikawa M, Hashimoto J, Hirokawa T, Sugimoto S, Kato T, Takagi M, Shin-Ya K. JBIR-22, an inhibitor for protein-protein interaction of the homodimer of proteasome assembly factor 3. Journal of natural products. 2010; 73:628–631.
34. Grigoreva TA, Tribulovich VG, Garabadzhiu AV, Melino G, Barlev NA. The 26S proteasome is a multifaceted target for anti-cancer therapies. *Oncotarget*. 2015;6(28):24733-24749.
35. Lin Y, Kang T, Zhou BP. Doxorubicin enhances Snail/LSD1-mediated PTEN suppression in a PARP1-dependent manner. *Cell Cycle*. 2014;13(11):1708-1716.
36. Gimm, O., Perren, A., Weng, L.-P., Marsh, D.J., Yeh, J.J., Ziebold, U., Gil, E., Hinze, R., Delbridge, L., Lees, J.A., et al. (2000). Differential nuclear and cytoplasmic expression of PTEN in normal thyroid tissue, and benign and malignant epithelial thyroid tumors. Am. J. Pathol. *156*, 1693–1700.
37. Ginn-Pease, M.E., and Eng, C. (2003). Increased nuclear phosphatase and tensin homologue deleted on chromosome 10 is associated with G0–G1 in MCF-7 cells. Cancer Res. *63*, 282–286.
38. Tachibana, M., Shibakita, M., Ohno, S., Kinugasa, S., Yoshimura, H., Ueda, S., Fujii, T., Rahman, M.A., Dhar, D.K., and Nagasue, N. (2002). Expression and prognostic significance of PTEN product protein in patients with esophageal squamous cell carcinoma. Cancer *94*, 1955–1960.
39. Trotman LC, Wang X, Alimonti A, et al. Ubiquitination regulates PTEN nuclear import and tumor suppression. *Cell*. 2007;128(1):141-156.
40. Depowski PL, Rosenthal SI, Ross JS. Loss of expression of the PTEN gene protein product is associated with poor outcome in breast cancer. *Mod Pathol*. 2001;14(7):672-676.
41. Dreher T, Zentgraf H, Abel U, et al. Reduction of PTEN and p27kip1 expression correlates with tumor grade in prostate cancer. analysis in radical prostatectomy specimens and needle biopsies. *Virchows Arch*. 2004;444(6):509-517.
42. Markson G, Kiel C, Hyde R, et al. Analysis of the human E2 ubiquitin conjugating enzyme protein interaction network. *Genome Res*. 2009;19(10):1905-1911.
43. Richert MM, Schwertfeger KL, Ryder JW, Anderson SM. An atlas of mouse mammary gland development. *J Mammary Gland Biol Neoplasia*. 2000;5(2):227-241.
44. Bromberg KD, Kluger HM, Delaunay A, et al. Increased expression of the E3 ubiquitin ligase RNF5 is associated with decreased survival in breast cancer. *Cancer Res*. 2007;67(17):8172-8179.